Robust energy a posteriori estimates for nonlinear elliptic problems

André Harnist, Koondanibha Mitra, Ari Rappaport, Martin Vohralík

Robust energy a posteriori estimates for nonlinear elliptic problems

André Harnist[†§*1] Koondanibha Mitra[‡2] Ari Rappaport[†§3] Martin Vohralík[†§4]

December 4, 2023

Abstract

In this paper, we design a posteriori estimates for finite element approximations of nonlinear elliptic problems satisfying strong-monotonicity and Lipschitz-continuity properties. These estimates include, and build on, any iterative linearization method that satisfies a few clearly identified assumptions; this encompasses the Picard, Newton, and Zarantonello linearizations. The estimates give a guaranteed upper bound on an augmented energy difference (reliability with constant one), as well as a lower bound (efficiency up to a generic constant). We prove that for the Zarantonello linearization, this generic constant only depends on the space dimension, the mesh shape regularity, and possibly the approximation polynomial degree in four or more space dimensions, making the estimates robust with respect to the strength of the nonlinearity. For the other linearizations, there is only a computable dependence on the local variation of the linearization operators. We also derive similar estimates for the energy difference. Numerical experiments illustrate and validate the theoretical results, for both smooth and singular solutions.

Key words: nonlinear elliptic problem, finite elements, iterative linearization, energy difference, a posteriori error estimate, robustness, equilibrated flux reconstruction

Contents

[1] andre.harnist@utc.fr, https://andreharnist.fr
[2] koondanibha.mitra@uhasselt.be, https://www.koondi.net
[3] ari.rappaport@inria.fr
[4] martin.vohralik@inria.fr, https://who.rocq.inria.fr/Martin.Vohralik
[†] Inria, 2 rue Simone Iff, 75589 Paris, France
[§] CERMICS, Ecole des Ponts, 77455 Marne-la-Vallée, France
[*] Current address: Laboratory of Applied Mathematics of Compiègne, CS 60319, Université de technologie de Compiègne, 60203 Compiègne, France
[‡] Hasselt University, Belgium

1 Introduction

Nonlinear elliptic problems are of paramount importance in a broad range of domains such as physics, mechanics, economics, biology, and medicine, see, e.g., [2, 22, 32, 41, 42]. Numerical discretization methods then serve to deliver approximate solutions, upon employing iterative linearizations to resolve the arising discrete nonlinear systems, see, e.g., [7, 16, 18, 29, 34, 45] and the references therein.

Given a numerical approximation, there arises the important question of the error with respect to the exact solution. This is practically handled by the so-called a posteriori estimates. For nonlinear problems, these have been proposed, amongst others, in [3, 4, 10, 11, 17, 20, 26, 28, 29, 33, 35, 37, 40, 41, 45]. In particular, already in, e.g., [45], the concept of a fully computable upper bound on the energy difference while relying on a duality gap has been discussed, see also [3, 4, 11, 26, 40, 41] and the references therein. The crucial question in this context is how to locally construct a suitable equilibrated flux. This has been a subject of research for several decades [36, 15, 38] and has only reached maturity recently [35, 8, 12, 20]. One step further, the estimates can be used to adaptively steer the numerical approximation, and recently, convergence and optimality results have been obtained in [5, 9, 24, 25, 27, 30, 31], see also the references therein.

Two crucial properties of an a posteriori estimate are the efficiency, assessing whether the estimate is not only an upper bound on the error, but also, up to a generic constant, a lower bound, and its robustness, assessing whether the quality of the estimate is independent of the parameters. In the present setting, we specifically use the term robustness if the chosen error measure and the associated estimate are uniformly equivalent, for any strength of the nonlinearity. Namely, the efficiency constant has to be indeed generic, independent of the strength of the nonlinearity, leading to the same overestimation factor (effectivity index) for linear, mildly nonlinear, and highly nonlinear problems. Unfortunately, robustness is typically (theoretically) not achieved; we illustrate this in Figure 1. There, we present the effectivity indices for three common error measures: the energy norm (L^2 norm of the difference of the weak gradients), the (square root of the) difference of the energies, and the dual norm of the residual (cf., e.g., [23] for their mutual comparisons). We employ guaranteed equilibrated flux estimates following [8, 20], for the problem of Example 6.2 below. We can observe that the estimate in the energy norm setting is not robust with respect to the strength of the nonlinearity (the effectivity index explodes as the ratio $a_\mathrm{c}/a_\mathrm{m}$ from (2.1) below grows). The dual norm of the residual leads to robustness, as proven in [17, 20]. Though the dual norm of the residual is indeed localizable, cf. [6] and the references therein, it may be criticized as it actually does not take into account the nonlinearity (an incorporation has recently been addressed in [39]). The energy difference then numerically shows a robustness, though, to the best of our knowledge, all known theoretical estimates, cf. the references above, depend unfavorably on the ratio $a_\mathrm{c}/a_\mathrm{m}$. Our main motivation in this context is to bring a theoretical insight to the robustness in the energy difference setting.

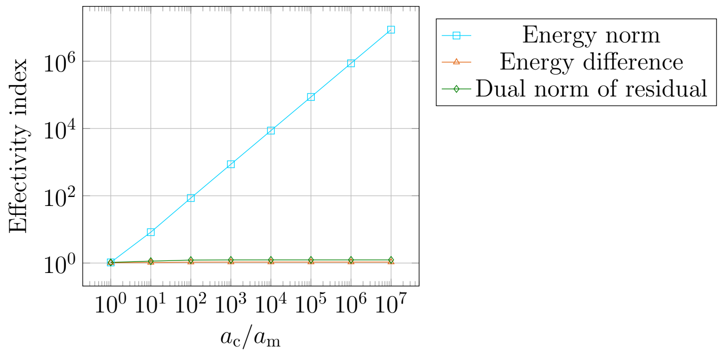

Figure 1: [Exponential nonlinearity (6.5), smooth solution (6.3), Newton solver, 25 DOFs] Comparison of the effectivity index (given as the ratio of the estimate over the error) of different error measures and associated a posteriori estimates.

We focus on nonlinear elliptic problems of the form: find $u : \Omega \to \mathbb{R}$ such that

$$-\boldsymbol{\nabla}\cdot(a(\cdot, |\boldsymbol{\nabla} u|)\boldsymbol{\nabla} u) = f \quad \text{in } \Omega, \tag{1.1a}$$

$$u = 0 \quad \text{on } \partial\Omega, \tag{1.1b}$$

where $a : \Omega \times [0, \infty) \to (0, \infty)$ is a nonlinear function satisfying assumptions of Lipschitz continuity and strong monotonicity (cf. (2.1) below). We employ a finite element approximation of (1.1) and an iterative linearization, yielding the approximation u_ℓ^k on each mesh $\mathcal{T}_\ell$ and linearization step k. The iterative linearization method needs to satisfy a few clearly identified assumptions. We will show that this is satisfied for usual linearizations such as Picard, Newton, or Zarantonello.

We consider the energy difference $\mathcal{E}_{\mathrm{N},\ell}^k$ of the nonlinear problem (cf. (4.1a)) and its a posteriori estimator $\eta_{\mathrm{N},\ell}^k$ (cf. (4.1b)). We establish that $\mathcal{E}_{\mathrm{N},\ell}^k$ and $\eta_{\mathrm{N},\ell}^k$ are respectively equivalent to L^2 norms of differences of the exact and approximate solutions with pointwise contributions of the nonlinearity (cf. Lemma 4.1). We then obtain our first main result, Theorem 4.4, which can be summarized as follows. For every iterative linearization index k, neglecting data oscillation, quadrature-type errors, and iterative linearization error terms, we have

$$\mathcal{E}_{\mathrm{N},\ell}^k \le \eta_{\mathrm{N},\ell}^k \lesssim C_\ell^k \mathcal{E}_{\mathrm{N},\ell}^k, \tag{1.2}$$

where the hidden constant depends only on the space dimension, the mesh shape-regularity, and possibly on the polynomial degree p of the finite element approximation when the spatial dimension is greater than or equal to 4. Here, C_ℓ^k only has a local, through unfortunately not computable, dependence on the nonlinearity; we prove that in any case, $C_\ell^k \le (a_\mathrm{c}/a_\mathrm{m})^{1/2}$.

In order to improve the above result and in particular the constant C_ℓ^k, we additionally consider a linearized energy difference $\mathcal{E}_{\mathrm{L},\ell}^k$ (cf. (5.2a)) and the associated estimator $\eta_{\mathrm{L},\ell}^k$ (cf. (5.2b)). We then augment $\mathcal{E}_{\mathrm{N},\ell}^k$ by $\mathcal{E}_{\mathrm{L},\ell}^k$ to form $\mathcal{E}_\ell^k$ and similarly for the estimators. We then obtain our second main result, Theorem 5.5, which can be presented as follows. For every iterative linearization index k, neglecting again data oscillation, quadrature-type errors, and iterative linearization error terms, we have

$$\mathcal{E}_\ell^k \le \eta_\ell^k \lesssim \widehat{C}_\ell^k \mathcal{E}_\ell^k, \tag{1.3}$$

with the same dependence as in (1.2) for the hidden constant. Here $\widehat{C}_\ell^k$ only depends on local variations of the linearization matrices and, crucially, is fully computable. Moreover, we show that $\widehat{C}_\ell^k = 1$ in the case of the Zarantonello linearization, making the estimate (1.3) robust with respect to the strength of the nonlinearity. For the other linearizations, the estimate (1.3) is robust if the computed constant $\widehat{C}_\ell^k$ is small, which is an a posteriori verification of robustness for each given setting (nonlinear function a, domain Ω, datum f, mesh $\mathcal{T}_\ell$, linearization step k, polynomial degree p). We also discuss in Remark 5.7 why we can expect $\widehat{C}_\ell^k$ tend to 1 in the discretization limit (ℓ large enough).

The rest of the paper is organized as follows. In Section 2, we detail the assumptions on the nonlinear function a. We next give the continuous weak formulation with its equivalent energy minimization. Then, we introduce the discrete weak formulation with its associated discrete energy minimization, and finally the iterative linearization. In Section 3, we define the convex conjugate, the duality setting, and the equilibrated flux necessary for our a posteriori estimates. In Section 4, we study the original energy difference, which leads us to our first main result, Theorem 4.4, giving details of (1.2). In Section 5, we define the augmented energy difference and estimator and state our second main result, Theorem 5.5, giving details of (1.3). In Section 6, we present a series of numerical experiments in order to illustrate our theoretical findings, for both settings (1.2) and (1.3) as well as smooth and singular solutions. In Section 7, we give a proof of crucial technical result of Lemma 4.1, and then in Section 8, a proof of Theorem 4.4. In Section 9, we give a proof of the boundedness of the weight λ_ℓ^k from Lemma 5.1 and of the augmented energy difference consistency summarized in Lemma 5.3, and then, in Section 10, a proof of Theorem 5.5. Finally, we summarize, in Appendix A, some useful properties of the nonlinear functions and the assumptions required, and, in Appendix B, we show some technical results to determine the local eigenvalues of the Newton linearization.

2 Weak formulation, energy minimization, finite element discretization, and iterative linearization

Let $\Omega \subset \mathbb{R}^d$, $d \geq 1$, be an open polytope with Lipschitz boundary $\partial\Omega$. We consider problem (1.1), where $f \in L^2(\Omega)$ represents a volumetric force term, while a is the diffusion coefficient which depends on the potential $u : \Omega \to \mathbb{R}$ only through the Euclidean norm of its gradient $|\nabla u|$.

We consider the following assumption for the nonlinear function a (see, e.g., [45] for more details).

Assumption 2.1 (Nonlinear function a)**.** *We assume that the function $a : \Omega \times [0, \infty) \to (0, \infty)$ is measurable and that there exist constants $a_{\mathrm{m}} \leq a_{\mathrm{c}} \in (0, \infty)$ such that, a.e. in Ω and for all $\boldsymbol{x}, \boldsymbol{y} \in \mathbb{R}^d$,*

$$|a(\cdot, |\boldsymbol{x}|)\boldsymbol{x} - a(\cdot, |\boldsymbol{y}|)\boldsymbol{y}| \leq a_{\mathrm{c}}|\boldsymbol{x} - \boldsymbol{y}| \qquad \textit{(Lipschitz continuity)}, \tag{2.1a}$$

$$(a(\cdot, |\boldsymbol{x}|)\boldsymbol{x} - a(\cdot, |\boldsymbol{y}|)\boldsymbol{y}) \cdot (\boldsymbol{x} - \boldsymbol{y}) \geq a_{\mathrm{m}}|\boldsymbol{x} - \boldsymbol{y}|^2 \qquad \textit{(strong monotonicity)}. \tag{2.1b}$$

2.1 Weak formulation and equivalent energy minimization

The weak formulation of problem (1.1) reads: find $u \in H_0^1(\Omega)$ such that

$$(a(\cdot, |\nabla u|)\nabla u, \nabla v) = (f, v) \qquad \forall v \in H_0^1(\Omega), \tag{2.2a}$$

where $(\cdot, \cdot)$ is the inner product of $L^2(\Omega)$.

Referring to [45], the weak formulation (2.2a) is equivalent to the following minimization problem:

$$u = \arg \min_{v \in H_0^1(\Omega)} \mathcal{J}(v), \tag{2.2b}$$

with the energy functional $\mathcal{J} : H_0^1(\Omega) \to \mathbb{R}$ defined as,

$$\mathcal{J}(v) := \int_\Omega \phi(\cdot, |\nabla v|) - (f, v), \quad v \in H_0^1(\Omega), \tag{2.3}$$

where the function $\phi : \Omega \times [0, \infty) \to [0, \infty)$ is defined such that, a.e. in Ω and for all $r \in [0, \infty)$,

$$\phi(\cdot, r) := \int_0^r a(\cdot, s)s \,\mathrm{d}s. \tag{2.4}$$

It is shown in [45] that, under Assumption 2.1, there exists a unique solution to problem (2.2). We refer to Appendix A for more details about equivalent assumptions on the nonlinear functions a and ϕ.

2.2 Finite element discretization

Let $\ell \geq 0$ be a mesh level index. We consider simplicial triangulations $\mathcal{T}_\ell$ of the domain Ω satisfying the following shape-regularity property: there exists a constant $\kappa_{\mathcal{T}} > 0$ such that for all $\ell \geq 0$ and all $K \in \mathcal{T}_\ell$, $h_K/\rho_K \leq \kappa_{\mathcal{T}}$, where h_K is the diameter of K and ρ_K is the diameter of the largest ball inscribed in K.

For a polynomial degree $p \geq 1$, denoting $\mathcal{P}_p(\mathcal{T}_\ell)$ the space of piecewise polynomials on the mesh $\mathcal{T}_\ell$ of total degree at most p, we define the discrete finite element space $V_\ell^p := \mathcal{P}_p(\mathcal{T}_\ell) \cap H_0^1(\Omega)$. The finite element approximation of (2.2a) would be $u_\ell \in V_\ell^p$ such that

$$(a(\cdot, |\nabla u_\ell|)\nabla u_\ell, \nabla v_\ell) = (f, v_\ell) \qquad \forall v_\ell \in V_\ell^p. \tag{2.5a}$$

As in (2.2b), $u_\ell \in V_\ell^p$ solves the minimization problem

$$u_\ell = \arg \min_{v_\ell \in V_\ell^p} \mathcal{J}(v_\ell). \tag{2.5b}$$

Below, we never work with u_ℓ but rather with its approximations coming from iterative linearization.

2.3 Iterative linearization

We henceforth consider an iterative linearization of (2.5a), which is anyhow necessary for a practical solution of (2.5a). Let $u_\ell^0 \in V_\ell^p$ be a given initial guess. For an iterative linearization index $k \geq 1$, consider $\boldsymbol{A}_\ell^{k-1} : \Omega \to \mathbb{R}^{d\times d}$ and $\boldsymbol{b}_\ell^{k-1} : \Omega \to \mathbb{R}^d$, arising from a suitable linearization; details and examples are given below. We define the linearized finite element approximation: $u_\ell^k \in V_\ell^p$ to be such that

$$(\boldsymbol{A}_\ell^{k-1}\boldsymbol{\nabla} u_\ell^k, \boldsymbol{\nabla} v_\ell) = (f, v_\ell) + (\boldsymbol{b}_\ell^{k-1}, \boldsymbol{\nabla} v_\ell) \qquad \forall v_\ell \in V_\ell^p. \tag{2.6a}$$

As in (2.5b), this is equivalent to the discrete minimization problem

$$u_\ell^k = \arg\min_{v_\ell \in V_\ell^p} \ \mathcal{J}_\ell^{k-1}(v_\ell) \tag{2.6b}$$

with the linearized energy functional $\mathcal{J}_\ell^{k-1} : H_0^1(\Omega) \to \mathbb{R}$ defined for all $v \in H_0^1(\Omega)$ by

$$\mathcal{J}_\ell^{k-1}(v) := \frac{1}{2}\left\|(\boldsymbol{A}_\ell^{k-1})^{\frac{1}{2}}\boldsymbol{\nabla} v\right\|^2 - (f, v) - (\boldsymbol{b}_\ell^{k-1}, \boldsymbol{\nabla} v), \tag{2.7}$$

where $\|\cdot\|$ is the $L^2(\Omega)$ norm corresponding to the inner product $(\cdot,\cdot)$ of $L^2(\Omega)$.

2.3.1 Assumptions on iterative linearization schemes

Let $k \geq 1$. We will suppose that $\boldsymbol{A}_\ell^{k-1} : \Omega \to \mathbb{R}^{d\times d}$ and $\boldsymbol{b}_\ell^{k-1} : \Omega \to \mathbb{R}^d$ from (2.6) satisfy Assumption 2.2 below (for the sake of conciseness, we assume that they are well defined everywhere in Ω). We will use the following notation of the derivatives in the second argument of the functions a, ϕ, and others (cf. (3.2)–(3.3)): for all $r \in [0,\infty)$, $a'(\cdot, r) := \frac{\partial}{\partial r} a(\boldsymbol{x}, r)$ and $\phi'(\cdot, r) := \frac{\partial}{\partial r}\phi(\boldsymbol{x}, r)$.

Assumption 2.2 (Iterative linearization)**.** *For all points $\boldsymbol{x} \in \Omega$, we assume that $\boldsymbol{A}_\ell^{k-1}(\boldsymbol{x}) \in \mathbb{R}^{d\times d}$ is a bounded symmetric positive definite matrix. Specifically, denoting by $A_{\mathrm{m},\ell}^{k-1}(\boldsymbol{x})$ and $A_{\mathrm{c},\ell}^{k-1}(\boldsymbol{x})$ respectively its smallest and largest pointwise eigenvalues, we have, for all $\boldsymbol{\xi} \in \mathbb{R}^d$,*

$$|\boldsymbol{A}_\ell^{k-1}(\boldsymbol{x})\boldsymbol{\xi}| \leq A_{\mathrm{c},\ell}^{k-1}(\boldsymbol{x})|\boldsymbol{\xi}| \quad \textit{(boundedness)}, \tag{2.8a}$$

$$(\boldsymbol{A}_\ell^{k-1}(\boldsymbol{x})\boldsymbol{\xi})\cdot\boldsymbol{\xi} \geq A_{\mathrm{m},\ell}^{k-1}(\boldsymbol{x})|\boldsymbol{\xi}|^2 \quad \textit{(positive definiteness)}. \tag{2.8b}$$

Moreover, we suppose uniformity, i.e., that there exist $A_\mathrm{m} \leq A_\mathrm{c} \in (0,\infty)$ independent of k, ℓ, and $\boldsymbol{x}$ such that

$$A_\mathrm{m} \leq A_{\mathrm{m},\ell}^{k-1}(\boldsymbol{x}) \leq A_{\mathrm{c},\ell}^{k-1}(\boldsymbol{x}) \leq A_\mathrm{c}. \tag{2.8c}$$

Finally, we explicitly define $\boldsymbol{b}_\ell^{k-1}(\boldsymbol{x}) \in \mathbb{R}^d$ for all $\boldsymbol{x} \in \Omega$ by

$$\boldsymbol{b}_\ell^{k-1}(\boldsymbol{x}) := \boldsymbol{A}_\ell^{k-1}(\boldsymbol{x})\boldsymbol{\nabla} u_\ell^{k-1}(\boldsymbol{x}) - a(\boldsymbol{x}, |\boldsymbol{\nabla} u_\ell^{k-1}(\boldsymbol{x})|)\boldsymbol{\nabla} u_\ell^{k-1}(\boldsymbol{x}). \tag{2.9}$$

In the following, we use the boldface font to denote the spaces of multi-dimensional functions, e.g., $\boldsymbol{L}^2(\Omega)$.

Remark 2.3 (Assumption 2.2)**.** *Equality (2.9) implies that (2.6a) can be equivalently written as a problem for the increment $u_\ell^k - u_\ell^{k-1}$ on the left-hand side and the residual of u_ℓ^{k-1} on the right-hand side:*

$$(\boldsymbol{A}_\ell^{k-1}\boldsymbol{\nabla}(u_\ell^k - u_\ell^{k-1}), \boldsymbol{\nabla} v_\ell) = (f, v_\ell) - (a(\cdot, |\boldsymbol{\nabla} u_\ell^{k-1}|)\boldsymbol{\nabla} u_\ell^{k-1}, \boldsymbol{\nabla} v_\ell) \ \ \forall v_\ell \in V_\ell^p, \tag{2.10}$$

which is the form used in, e.g., [39]. Therefore, equality (2.9) ensures that the discrete problem (2.6a) is consistent with the discrete problem (2.5a) in that

$$\boldsymbol{A}_\ell^{k-1}\boldsymbol{\nabla} u_\ell^k - \boldsymbol{b}_\ell^{k-1} \to a(\cdot, |\boldsymbol{\nabla} u_\ell|)\boldsymbol{\nabla} u_\ell \ \textit{in}\ \boldsymbol{L}^2(\Omega) \quad \textit{when} \quad u_\ell^k \to u_\ell \ \textit{in}\ H_0^1(\Omega). \tag{2.11}$$

Indeed, (2.8a) and (2.8c) imply that $\boldsymbol{A}_\ell^{k-1}\boldsymbol{\nabla}(u_\ell^k - u_\ell^{k-1}) \to \boldsymbol{0}$ in $\boldsymbol{L}^2(\Omega)$, whereas $a(\cdot, |\boldsymbol{\nabla} u_\ell^{k-1}|)\boldsymbol{\nabla} u_\ell^{k-1} \to a(\cdot, |\boldsymbol{\nabla} u_\ell|)\boldsymbol{\nabla} u_\ell$ in $\boldsymbol{L}^2(\Omega)$ thanks to (2.1a). Finally, we recall that the positive definiteness of $\boldsymbol{A}_\ell^{k-1}$ implies that $(\boldsymbol{A}_\ell^{k-1})^{-1}$ and $(\boldsymbol{A}_\ell^{k-1})^{\frac{1}{2}}$ exist, which is used below.

2.3.2 Examples of iterative linearization schemes

We now present some examples of linearization methods satisfying Assumption 2.2.

Example 2.4 (Picard)**.** *The Picard (fixed point) iteration, see, e.g., [16], is defined as*

$$\boldsymbol{A}_\ell^{k-1} = a(\cdot, |\boldsymbol{\nabla} u_\ell^{k-1}|)\boldsymbol{I}_d \quad \textit{with} \quad \boldsymbol{b}_\ell^{k-1} = \boldsymbol{0} \quad \textit{in } \Omega. \tag{2.12}$$

It satisfies Assumption 2.2 with $A_{\mathrm{m},\ell}^{k-1} = A_{\mathrm{c},\ell}^{k-1} = a(\cdot, |\boldsymbol{\nabla} u_\ell^{k-1}|)$*, which leads to* $A_\mathrm{m} = a_\mathrm{m}$ *and* $A_\mathrm{c} = a_\mathrm{c}$ *thanks to* (A.3).

Example 2.5 (Zarantonello)**.** *The Zarantonello iteration, introduced in [44], is defined as*

$$\boldsymbol{A}_\ell^{k-1} = \gamma \boldsymbol{I}_d \quad \textit{with} \quad \boldsymbol{b}_\ell^{k-1} = \big(\gamma - a(\cdot, |\boldsymbol{\nabla} u_\ell^{k-1}|)\big) \boldsymbol{\nabla} u_\ell^{k-1} \quad \textit{in } \Omega, \tag{2.13}$$

where $\gamma \in (0, \infty)$ *is a constant parameter. To ensure contraction, one needs to assume that* $\gamma \geq \frac{a_\mathrm{c}^2}{a_\mathrm{m}}$*. The Zarantonello iteration maintains the same linearization matrix* $\gamma \boldsymbol{I}_d$ *during the iterations and converges linearly, but the convergence is slow as* γ *takes large values. It satisfies Assumption 2.2 with* $A_{\mathrm{m},\ell}^{k-1} = A_{\mathrm{c},\ell}^{k-1} = \gamma$*, which leads to* $A_\mathrm{m} = A_\mathrm{c} = \gamma$*.*

Example 2.6 ((Damped) Newton)**.** *The (damped) Newton iteration, see, e.g., [16], is defined as*

$$\begin{aligned} \boldsymbol{A}_\ell^{k-1} &= a(\cdot, |\boldsymbol{\nabla} u_\ell^{k-1}|)\boldsymbol{I}_d + \theta \frac{a'(\cdot, |\boldsymbol{\nabla} u_\ell^{k-1}|)}{|\boldsymbol{\nabla} u_\ell^{k-1}|} \boldsymbol{\nabla} u_\ell^{k-1} \otimes \boldsymbol{\nabla} u_\ell^{k-1} \\ \textit{with } \boldsymbol{b}_\ell^{k-1} &= \theta a'(\cdot, |\boldsymbol{\nabla} u_\ell^{k-1}|)|\boldsymbol{\nabla} u_\ell^{k-1}|\boldsymbol{\nabla} u_\ell^{k-1} \quad \textit{in } \Omega, \end{aligned} \tag{2.14}$$

where $\theta \in [0,1]$ *is the damping parameter. Observe that* $\theta = 1$ *gives the Newton iteration, whereas* $\theta = 0$ *corresponds to the Picard iteration. If* $\theta = 1$*, the Newton method converges quadratically. However, it might not always converge. The (damped) Newton iteration satisfies Assumption 2.2 with, if the space dimension* $d = 1$*,*

$$\begin{aligned} A_{\mathrm{m},\ell}^{k-1} = A_{\mathrm{c},\ell}^{k-1} &= a(\cdot, |\boldsymbol{\nabla} u_\ell^{k-1}|) + \theta a'(\cdot, |\boldsymbol{\nabla} u_\ell^{k-1}|)|\boldsymbol{\nabla} u_\ell^{k-1}| \\ &\overset{(A.8)}{=} (1-\theta) a(\cdot, |\boldsymbol{\nabla} u_\ell^{k-1}|) + \theta \phi''(\cdot, |\boldsymbol{\nabla} u_\ell^{k-1}|), \end{aligned} \tag{2.15}$$

and, if $d > 1$*,*

$$A_{\mathrm{m},\ell}^{k-1} = (1-\theta) a(\cdot, |\boldsymbol{\nabla} u_\ell^{k-1}|) + \theta \min(a(\cdot, |\boldsymbol{\nabla} u_\ell^{k-1}|), \phi''(\cdot, |\boldsymbol{\nabla} u_\ell^{k-1}|)), \tag{2.16a}$$

$$A_{\mathrm{c},\ell}^{k-1} = (1-\theta) a(\cdot, |\boldsymbol{\nabla} u_\ell^{k-1}|) + \theta \max(a(\cdot, |\boldsymbol{\nabla} u_\ell^{k-1}|), \phi''(\cdot, |\boldsymbol{\nabla} u_\ell^{k-1}|)). \tag{2.16b}$$

Indeed, denoting the spectrum of a matrix $\boldsymbol{A} \in \mathbb{R}^{d \times d}$ *by* $\mathrm{Spec}(\boldsymbol{A})$*, we infer* (2.16) *by writing,*

$$\begin{aligned} \mathrm{Spec}(\boldsymbol{A}_\ell^{k-1}) &\overset{(B.1)}{=} \{a(\cdot, |\boldsymbol{\nabla} u_\ell^{k-1}|), a(\cdot, |\boldsymbol{\nabla} u_\ell^{k-1}|) + \theta a'(\cdot, |\boldsymbol{\nabla} u_\ell^{k-1}|)|\boldsymbol{\nabla} u_\ell^{k-1}|\} \\ &\overset{(A.8)}{=} \{(1-\theta) a(\cdot, |\boldsymbol{\nabla} u_\ell^{k-1}|) + \theta a(\cdot, |\boldsymbol{\nabla} u_\ell^{k-1}|), \\ &\qquad (1-\theta) a(\cdot, |\boldsymbol{\nabla} u_\ell^{k-1}|) + \theta \phi''(\cdot, |\boldsymbol{\nabla} u_\ell^{k-1}|)\}. \end{aligned}$$

Finally, we can set $A_\mathrm{m} = a_\mathrm{m}$ *and* $A_\mathrm{c} = a_\mathrm{c}$ *thanks to* (A.3) *and* (A.5).

3 Convex conjugate, dual energy, and flux equilibration

In this section, we define some common tools for the forthcoming developments.

3.1 Convex conjugate function and dual energy

Recalling the primal energy $\mathcal{J}$ of (2.3), the corresponding dual energy $\mathcal{J}^* : \boldsymbol{H}(\mathrm{div}, \Omega) \to \mathbb{R}$, cf. [2, 32, 41, 45], is defined by

$$\mathcal{J}^*(\boldsymbol{w}) := -\int_\Omega \phi^*(\cdot, |\boldsymbol{w}|), \quad \boldsymbol{w} \in \boldsymbol{H}(\mathrm{div}, \Omega), \tag{3.1}$$

where $\phi^* : \Omega \times [0,\infty) \to [0,\infty)$ is the convex conjugate of ϕ (also known as the Legendre dual or the Fenchel conjugate), which is defined such that, a.e. in Ω and for all $s \in [0,\infty)$,

$$\phi^*(\cdot, s) := \sup_{r\in[0,\infty)} (sr - \phi(\cdot, r)), \tag{3.2a}$$

or equivalently, for all $s \in [0,\infty)$,

$$\phi^*(\cdot, s) = \int_0^s {\phi'}^{-1}(\cdot, r)\,\mathrm{d}r = s{\phi'}^{-1}(\cdot, s) - \phi(\cdot, {\phi'}^{-1}(\cdot, s)). \tag{3.2b}$$

We refer to [32] for more details and recall that the construction of ϕ^* yields

$$\phi^{*\prime} = {\phi'}^{-1} \quad \text{and} \quad \phi^{*\prime\prime} = \frac{1}{\phi'' \circ {\phi'}^{-1}}. \tag{3.3}$$

Consequently, under Assumption 2.1, ϕ^* is convex thanks to Remark A.3 below.

Finally, we define the linearized dual energy functional $\mathcal{J}_\ell^{*,k-1} : \boldsymbol{H}(\mathrm{div}, \Omega) \to \mathbb{R}$ such that

$$\mathcal{J}_\ell^{*,k-1}(\boldsymbol{w}) := -\frac{1}{2}\left\|(\boldsymbol{A}_\ell^{k-1})^{-\frac{1}{2}}(\boldsymbol{w} - \boldsymbol{b}_\ell^{k-1})\right\|^2, \quad \boldsymbol{w} \in \boldsymbol{H}(\mathrm{div}, \Omega). \tag{3.4}$$

3.2 Flux equilibration

Let $\mathcal{V}_\ell$ be the set of all mesh vertices and, for each vertex $\boldsymbol{a} \in \mathcal{V}_\ell$, define the patch $\mathcal{T}_\ell^{\boldsymbol{a}}$ as the collection of the simplicies of $\mathcal{T}_\ell$ sharing the vertex $\boldsymbol{a}$, as well as the patch subdomain $\omega_\ell^{\boldsymbol{a}}$ corresponding to $\mathcal{T}_\ell^{\boldsymbol{a}}$. For all $\boldsymbol{a} \in \mathcal{V}_\ell$, we define the space $\boldsymbol{V}_\ell^{\boldsymbol{a}} := \boldsymbol{RTN}_p(\mathcal{T}_\ell^{\boldsymbol{a}}) \cap \boldsymbol{H}_0(\mathrm{div}, \omega_\ell^{\boldsymbol{a}})$. Here $\boldsymbol{RTN}_p(\mathcal{T}_\ell^{\boldsymbol{a}})$ denotes the broken space consisting of p-th order Raviart–Thomas–Nédélec space on each simplex, $\boldsymbol{RTN}_p(K) := [\mathcal{P}_p(K)]^d + \boldsymbol{x}\mathcal{P}_p(K)$. Moreover, $\boldsymbol{H}_0(\mathrm{div}, \omega_\ell^{\boldsymbol{a}})$ is the subspace of $\boldsymbol{H}(\mathrm{div}, \omega_\ell^{\boldsymbol{a}})$ of functions with vanishing normal trace on $\partial\omega_\ell^{\boldsymbol{a}}$ if $\boldsymbol{a} \in \mathcal{V}_\ell$ is an interior vertex and of functions with vanishing normal trace on $\partial\omega_\ell^{\boldsymbol{a}} \backslash \{\psi_\ell^{\boldsymbol{a}} > 0\}$ if $\boldsymbol{a} \in \mathcal{V}_\ell$ is a boundary vertex. Here, for all $\boldsymbol{a} \in \mathcal{V}_\ell$, the hat function $\psi_\ell^{\boldsymbol{a}}$ is the continuous, piecewise affine function equal to 1 in $\boldsymbol{a}$ and 0 in $\mathcal{V}_\ell \backslash \{\boldsymbol{a}\}$. We recall the partition of unity

$$\sum_{\boldsymbol{a}\in\mathcal{V}_\ell} \psi_\ell^{\boldsymbol{a}}(\boldsymbol{x}) = 1 \quad \forall \boldsymbol{x} \in \Omega. \tag{3.5}$$

We denote by $\Pi_{\ell,p}$ the L^2-orthogonal projection from $L^2(\Omega)$ to $\mathcal{P}_p(\mathcal{T}_\ell)$ and by $\boldsymbol{\Pi}_{\ell,p-1}^{\boldsymbol{RTN}}$ the $\boldsymbol{L}^2$-orthogonal projection from $\boldsymbol{L}^2(\Omega)$ to $\boldsymbol{RTN}_{p-1}(\mathcal{T}_\ell)$; note that both are elementwise. Finally, we consider the equilibrated flux locally reconstructed from u_ℓ^k as

$$\boldsymbol{\sigma}_\ell^k := \sum_{\boldsymbol{a}\in\mathcal{V}_\ell} \boldsymbol{\sigma}_\ell^{\boldsymbol{a},k}, \tag{3.6a}$$

where, for all vertices $\boldsymbol{a} \in \mathcal{V}_\ell$, following [8, 11, 15, 20, 21],

$$\begin{aligned} \boldsymbol{\sigma}_\ell^{\boldsymbol{a},k} &:= \arg \min_{\substack{\boldsymbol{w}_\ell \in \boldsymbol{V}_\ell^{\boldsymbol{a}} \\ \boldsymbol{\nabla}\cdot\boldsymbol{w}_\ell = \Pi_{\ell,p}\gamma_\ell^{\boldsymbol{a},k}}} \|(\boldsymbol{\Upsilon}_\ell^k)^{-\frac{1}{2}}(\psi_\ell^{\boldsymbol{a}}\boldsymbol{\Pi}_{\ell,p-1}^{\boldsymbol{RTN}}\boldsymbol{\xi}_\ell^k + \boldsymbol{w}_\ell)\|_{\omega_\ell^{\boldsymbol{a}}}, \\ \text{with } \boldsymbol{\xi}_\ell^k &:= \boldsymbol{A}_\ell^{k-1}\boldsymbol{\nabla}u_\ell^k - \boldsymbol{b}_\ell^{k-1}, \quad \gamma_\ell^{\boldsymbol{a},k} := \psi_\ell^{\boldsymbol{a}} f - \boldsymbol{\nabla}\psi_\ell^{\boldsymbol{a}} \cdot \boldsymbol{\xi}_\ell^k \end{aligned} \tag{3.6b}$$

and where the weight $\boldsymbol{\Upsilon}_\ell^k$ will be chosen according to needs. Specifically, we will set

$$\boldsymbol{\Upsilon}_\ell^k := \boldsymbol{I}_d \text{ in Section 4}, \tag{3.7a}$$

$$\boldsymbol{\Upsilon}_\ell^k := \boldsymbol{A}_\ell^{k-1} \text{ in Section 5}. \tag{3.7b}$$

We note that

$$(\gamma_\ell^{\boldsymbol{a},k}, 1)_{\omega_\ell^{\boldsymbol{a}}} = 0$$

for all interior vertices $\boldsymbol{a} \in \mathcal{V}_\ell$, which is an immediate consequence of (2.6a) with the test function $v_\ell = \psi_\ell^{\boldsymbol{a}} \in V_\ell^p$. Consequently, problems (3.6b) are well posed.

Combining (3.6) and (3.5), we infer, as in, e.g., [19],

$$\begin{aligned}\nabla\cdot\boldsymbol{\sigma}_\ell^k &= \sum_{\boldsymbol{a}\in\mathcal{V}_\ell}\nabla\cdot\boldsymbol{\sigma}_\ell^{\boldsymbol{a},k} = \sum_{\boldsymbol{a}\in\mathcal{V}_\ell}\Pi_{\ell,p}(\psi_\ell^{\boldsymbol{a}}f) - \sum_{\boldsymbol{a}\in\mathcal{V}_\ell}\Pi_{\ell,p}(\nabla\psi_\ell^{\boldsymbol{a}}\cdot\boldsymbol{\xi}_\ell^k)\\ &= \Pi_{\ell,p}\sum_{\boldsymbol{a}\in\mathcal{V}_\ell}(\psi_\ell^{\boldsymbol{a}}f) = \Pi_{\ell,p}f.\end{aligned} \tag{3.8}$$

In particular, $\boldsymbol{\sigma}_\ell^k \in \boldsymbol{RTN}_p(\mathcal{T}_\ell)\cap\boldsymbol{H}(\mathrm{div},\Omega)$ and we have with the Green theorem, since $u_\ell^k \in V_\ell^p = \mathcal{P}_p(\mathcal{T}_\ell)\cap H_0^1(\Omega)$,

$$-(\boldsymbol{\sigma}_\ell^k, \nabla u_\ell^k) = (f, u_\ell^k). \tag{3.9}$$

4 A posteriori estimate of the energy difference

This section gives an a posteriori estimate of the energy difference.

4.1 Energy difference and the associated estimator

We define the (square root of twice the) energy difference corresponding to the nonlinear problem (2.2) by

$$\mathcal{E}_{\mathrm{N},\ell}^k := \left(2(\mathcal{J}(u_\ell^k) - \mathcal{J}(u))\right)^{\frac{1}{2}}. \tag{4.1a}$$

Note that $\mathcal{E}_{\mathrm{N},\ell}^k$ is well defined from (2.2b) and the fact that $u_\ell^k \in H_0^1(\Omega)$. Actually, $\mathcal{E}_{\mathrm{N},\ell}^k \geq 0$ and 0 if and only if $u_\ell^k = u$ from the uniqueness of u in (2.2b). We then define the estimator $\eta_{\mathrm{N},\ell}^k$ corresponding to the nonlinear problem (2.2) as in, e.g., [3, 41, 45], employing the dual energy $\mathcal{J}^*$ of (3.1) and the equilibrated flux $\boldsymbol{\sigma}_\ell^k$ of (3.6) with the choice (3.7a),

$$\eta_{\mathrm{N},\ell}^k := \left(2(\mathcal{J}(u_\ell^k) - \mathcal{J}^*(\boldsymbol{\sigma}_\ell^k))\right)^{\frac{1}{2}}. \tag{4.1b}$$

Note that $\eta_{\mathrm{N},\ell}^k$ is well defined (the argument of the square root is nonnegative), which can be seen from (6.7)–(6.8) below.

4.2 Locally-weighted bounds for the energy difference and the associated estimator

Denoting, a.e. in Ω,

$$a_\ell^k := a(\cdot, |\nabla u_\ell^k|) \quad \text{and} \quad a_u := a(\cdot, |\nabla u|), \tag{4.2}$$

we define, for all $(v, \boldsymbol{w}) \in L^1(\Omega)\times[L^1(\Omega)]^d$, a.e. in Ω,

$$a_{\mathrm{m},\ell}^k(v,\boldsymbol{w}) := \min\left(a(\cdot,|\nabla v|), \operatorname*{ess\,inf}_{r\in(|\boldsymbol{w}|,|a_\ell^k\nabla u_\ell^k|)}\phi''(\cdot,\phi'^{-1}(\cdot,r))\right) \overset{(A.3),(A.5)}{\in} [a_{\mathrm{m}}, a_{\mathrm{c}}], \tag{4.3a}$$

$$a_{\mathrm{c},\ell}^k(v,\boldsymbol{w}) := \max\left(a(\cdot,|\nabla v|), \operatorname*{ess\,sup}_{r\in(|\boldsymbol{w}|,|a_\ell^k\nabla u_\ell^k|)}\phi''(\cdot,\phi'^{-1}(\cdot,r))\right) \overset{(A.3),(A.5)}{\in} [a_{\mathrm{m}}, a_{\mathrm{c}}], \tag{4.3b}$$

and, for the sake of brevity, we denote for both $\alpha \in \{\mathrm{m},\mathrm{c}\}$, a.e. in Ω,

$$a_{\alpha,\ell}^{\boldsymbol{\sigma},k} := a_{\alpha,\ell}^k(u_\ell^k, \boldsymbol{\sigma}_\ell^k), \quad a_{\alpha,\ell}^{\nabla u,k} := a_{\alpha,\ell}^k(u_\ell^k, a_u\nabla u), \quad \text{and} \quad a_{\alpha,\ell}^{u,k} := a_{\alpha,\ell}^k(u, a_u\nabla u). \tag{4.3c}$$

Observe that $a_{\mathrm{m},\ell}^{\boldsymbol{\sigma},k}$ and $a_{\mathrm{c},\ell}^{\boldsymbol{\sigma},k}$ are computable, in contrast to the other terms in (4.3c).

Lemma 4.1 (Locally-weighted bounds for the energy difference and estimator)**.** *Recalling* (4.1)–(4.3), *we have*

$$\|(a_{\mathrm{m},\ell}^{u,k})^{\frac{1}{2}}(\nabla u_\ell^k - \nabla u)\|^2 \leq (\mathcal{E}_{\mathrm{N},\ell}^k)^2 \leq \|(a_{\mathrm{c},\ell}^{u,k})^{\frac{1}{2}}(\nabla u_\ell^k - \nabla u)\|^2, \tag{4.4a}$$

$$\|(a_{\mathrm{c},\ell}^{\boldsymbol{\sigma},k})^{-\frac{1}{2}}(a_\ell^k\nabla u_\ell^k + \boldsymbol{\sigma}_\ell^k)\|^2 \leq (\eta_{\mathrm{N},\ell}^k)^2 \leq \|(a_{\mathrm{m},\ell}^{\boldsymbol{\sigma},k})^{-\frac{1}{2}}(a_\ell^k\nabla u_\ell^k + \boldsymbol{\sigma}_\ell^k)\|^2, \tag{4.4b}$$

$$\|(a_{\mathrm{c},\ell}^{\nabla u,k})^{-\frac{1}{2}}(a_\ell^k\nabla u_\ell^k - a_u\nabla u)\|^2 \leq (\mathcal{E}_{\mathrm{N},\ell}^k)^2 \leq 2\|(a_{\mathrm{m},\ell}^{\nabla u,k})^{-\frac{1}{2}}(a_\ell^k\nabla u_\ell^k - a_u\nabla u)\|^2. \tag{4.4c}$$

The proof of this important technical result is postponed to Section 7.

4.3 Data oscillation, quadrature-type, and iterative linearization estimators

Following, e.g, [19], let

$$(\eta_{\mathrm{osc},\ell}^k)^2 := \sum_{K\in\mathcal{T}_\ell}\left[\frac{h_K}{\pi a_{\mathrm{m}}^{\frac{1}{2}}}\|(I-\Pi_{\ell,p})f\|_K\right]^2, \tag{4.5a}$$

$$(\eta_{\mathrm{osc,q},\ell}^k)^2 := \sum_{\boldsymbol{a}\in\mathcal{V}_\ell}(\eta_{\mathrm{osc,q},\ell}^{\boldsymbol{a},k})^2 \quad\text{and}\quad (\eta_{\mathrm{iter},\ell}^k)^2 := \sum_{\boldsymbol{a}\in\mathcal{V}_\ell}(\eta_{\mathrm{iter},\ell}^{\boldsymbol{a},k})^2, \tag{4.5b}$$

where, for all vertices $\boldsymbol{a}\in\mathcal{V}_\ell$, recalling the notation from (3.6b),

$$(\eta_{\mathrm{osc,q},\ell}^{\boldsymbol{a},k})^2 := \frac{1}{\operatorname{ess\,inf}_{\omega_\ell^{\boldsymbol{a}}} a_{\mathrm{m},\ell}^{\boldsymbol{\sigma},k}}\left(\sum_{K\in\mathcal{T}_\ell^{\boldsymbol{a}}}\left[\frac{h_K}{\pi}\|(I-\Pi_{\ell,p})\gamma_\ell^{\boldsymbol{a},k}\|_K\right]^2 + \|\psi_\ell^{\boldsymbol{a}}(\boldsymbol{I}-\boldsymbol{\Pi}_{\ell,p-1}^{\boldsymbol{RTN}})\boldsymbol{\xi}_\ell^k\|_{\omega_\ell^{\boldsymbol{a}}}^2\right), \tag{4.5c}$$

$$(\eta_{\mathrm{iter},\ell}^{\boldsymbol{a},k})^2 := \frac{1}{\operatorname{ess\,inf}_{\omega_\ell^{\boldsymbol{a}}} a_{\mathrm{m},\ell}^{\boldsymbol{\sigma},k}}\|a_\ell^k\boldsymbol{\nabla}u_\ell^k - \boldsymbol{\xi}_\ell^k\|_{\omega_\ell^{\boldsymbol{a}}}^2. \tag{4.5d}$$

Remark 4.2 (Data oscillation and quadrature-type estimators). *The estimator $\eta_{\mathrm{osc},\ell}^k$ monitors the so-called oscillation in the source datum f: it vanishes if f is piecewise polynomial and is of higher order for piecewise smooth f. The quadrature-type estimators $\eta_{\mathrm{osc,q},\ell}^k$ arise from piecewise polynomial approximation of the (possibly) apolynomial data $\gamma_\ell^{\boldsymbol{a},k}$ and $\boldsymbol{\xi}_\ell^k$ defined in (3.6b), which involve themselves the nonlinear function a through $\boldsymbol{A}_\ell^{k-1}$ and $\boldsymbol{b}_\ell^{k-1}$, cf. Section 2.3.2. These terms can completely disappear (for the lowest polynomial degree $p=1$ where $a(\cdot,|\boldsymbol{\nabla}u_\ell^{k-1}|)$ and $a'(\cdot,|\boldsymbol{\nabla}u_\ell^{k-1}|)$ are piecewise constant if the spatial dependence in a is piecewise constant) or be of higher order if the nonlinear function a has the necessary smoothness. One could actually force them to be negligible if a separate, sufficiently increased polynomial degree was chosen for the equilibration in (3.6b).*

Remark 4.3 (Iterative linearization estimator). *Congruently with (2.11), if $u_\ell^k\to u_\ell$ in $H_0^1(\Omega)$, then we can have $\eta_{\mathrm{iter},\ell}^k$ as small as we need since, also using the standard coloring bound (8.3),*

$$\begin{aligned}\eta_{\mathrm{iter},\ell}^k &\overset{(4.3a),(3.6b),(2.9)}{\leq} a_{\mathrm{m}}^{-\frac{1}{2}}(d+1)\|a_\ell^k\boldsymbol{\nabla}u_\ell^k - a_\ell^{k-1}\boldsymbol{\nabla}u_\ell^{k-1} - \boldsymbol{A}_\ell^{k-1}\boldsymbol{\nabla}(u_\ell^k-u_\ell^{k-1})\| \\ &\overset{(2.1a),(2.8)}{\leq} a_{\mathrm{m}}^{-\frac{1}{2}}(d+1)(a_{\mathrm{c}}+A_{\mathrm{c}})\|\boldsymbol{\nabla}(u_\ell^k-u_\ell^{k-1})\|.\end{aligned} \tag{4.6}$$

4.4 A posteriori estimate of the energy difference

We now present our first main result, giving an a posteriori estimate for the energy difference $\mathcal{E}_{\mathrm{N},\ell}^k$ and the estimator $\eta_{\mathrm{N},\ell}^k$ defined in (4.1).

Theorem 4.4 (A posteriori estimate of the energy difference). *Suppose Assumption 2.1 and let $u\in H_0^1(\Omega)$ be the weak solution of (2.2). Let u_ℓ^k be its finite element approximation given by (2.6) on mesh $\mathcal{T}_\ell$, $\ell\geq 0$, and linearization step $k\geq 1$, for any iterative linearization satisfying Assumption 2.2. Let $\boldsymbol{\sigma}_\ell^k$ be the equilibrated flux defined by (3.6) with the choice (3.7a). Then*

$$\mathcal{E}_{\mathrm{N},\ell}^k \leq \eta_{\mathrm{N},\ell}^k + 2\eta_{\mathrm{osc},\ell}^k, \tag{4.7a}$$

$$\eta_{\mathrm{N},\ell}^k \lesssim C_\ell^k\mathcal{E}_{\mathrm{N},\ell}^k + \eta_{\mathrm{osc,q},\ell}^k + \eta_{\mathrm{iter},\ell}^k, \tag{4.7b}$$

where the hidden constant only depends on the space dimension d, the mesh shape-regularity $\kappa_{\mathcal{T}}$, and possibly, when $d\geq 4$, the polynomial degree p, with

$$C_\ell^k := \max_{\boldsymbol{a}\in\mathcal{V}_\ell}\left(\frac{\operatorname{ess\,sup}_{\omega_\ell^{\boldsymbol{a}}} a_{\mathrm{c},\ell}^{\boldsymbol{\nabla}u,k}}{\operatorname{ess\,inf}_{\omega_\ell^{\boldsymbol{a}}} a_{\mathrm{m},\ell}^{\boldsymbol{\sigma},k}}\right)^{\frac{1}{2}} \overset{(4.3)}{\leq} \left(\frac{a_{\mathrm{c}}}{a_{\mathrm{m}}}\right)^{\frac{1}{2}}. \tag{4.8}$$

Proof. See Section 8. □

Remark 4.5 (Structure of C_ℓ^k and robustness). *The constant C_ℓ^k from (4.8) is composed of purely local contributions. Since the ratios of $a_{\mathrm{c},\ell}^{\boldsymbol{\nabla}u,k}$ to $a_{\mathrm{m},\ell}^{\boldsymbol{\sigma},k}$ on each patch $\omega_\ell^{\boldsymbol{a}}$ are smaller than the global ratio $a_{\mathrm{c}}/a_{\mathrm{m}}$ and since the patches $\omega_\ell^{\boldsymbol{a}}$ shrink with mesh refinement, C_ℓ^k may converge to 1. For example, in the case* *where the problem is smooth in that $a \in C^1(\Omega \times [0,\infty))$, $u \in C^1(\Omega)$, and $\nabla u_\ell^k \to \nabla u$ in $[L^\infty(\Omega)]^d$, then, for ℓ and k large enough,*

$$C_\ell^k \overset{(4.3)}{\lesssim} \widetilde{C}_\ell^k \coloneqq \operatorname*{ess\,sup}_{\boldsymbol{x}\in\Omega} \left(\max\left(\frac{\phi''}{a}, \frac{a}{\phi''} \right)(\boldsymbol{x}, |\nabla u_\ell^k(\boldsymbol{x})|) \right)^{\frac{1}{2}}, \tag{4.9}$$

which is small if the function ϕ''/a is close to 1 over $\Omega \times [0,\infty)$. Unfortunately, C_ℓ^k from (4.8) cannot be computed and its value may possibly explode with the ratio $(a_{\mathrm{c}}/a_{\mathrm{m}})^{1/2}$.

In the next section, by augmenting the energy difference, we will achieve a result similar to (4.7) but with a computable constant C_ℓ^k which moreover takes value 1 for the Zarantonello linearization of Example 2.5.

5 A posteriori estimate of the augmented energy difference

This section gives an a posteriori estimate of the augmented energy difference defined below.

5.1 Energy difference and estimator of the linearized problem

In order to derive robust estimates, we now also crucially consider the linearized problem (2.6). We introduce the abstract linearization on the continuous level: find $u_{\langle\ell\rangle}^k \in H_0^1(\Omega)$ such that

$$(\boldsymbol{A}_\ell^{k-1} \nabla u_{\langle\ell\rangle}^k, \nabla v) = (f, v) + (\boldsymbol{b}_\ell^{k-1}, \nabla v) \qquad \forall v \in H_0^1(\Omega), \tag{5.1a}$$

which is a linear problem. Note that (5.1a) is equivalent to

$$u_{\langle\ell\rangle}^k \coloneqq \arg \min_{v \in H_0^1(\Omega)} \mathcal{J}_\ell^{k-1}(v), \tag{5.1b}$$

employing the linearized energy (2.7). Analogously to the (nonlinear) energy difference $\mathcal{E}_{\mathrm{N},\ell}^k$ (4.1a), we define the energy difference $\mathcal{E}_{\mathrm{L},\ell}^k$ of the linearized problem (5.1) as

$$\mathcal{E}_{\mathrm{L},\ell}^k \coloneqq \Big(2\big(\mathcal{J}_\ell^{k-1}(u_\ell^k) - \mathcal{J}_\ell^{k-1}(u_{\langle\ell\rangle}^k) \big) \Big)^{\frac{1}{2}} \overset{(10.1a)}{=} \|(\boldsymbol{A}_\ell^{k-1})^{\frac{1}{2}} \nabla(u_\ell^k - u_{\langle\ell\rangle}^k)\|. \tag{5.2a}$$

Here, there holds trivially $\mathcal{E}_{\mathrm{L},\ell}^k \geq 0$ and $\mathcal{E}_{\mathrm{L},\ell}^k = 0$ if and only if $u_\ell^k = u_{\langle\ell\rangle}^k$. Finally, we define the estimator $\eta_{\mathrm{L},\ell}^k$ of the linearized problem (5.1), employing the linearized dual energy (3.4) and the equilibrated flux $\boldsymbol{\sigma}_\ell^k$ of (3.6) with the choice (3.7b), by

$$\begin{aligned} \eta_{\mathrm{L},\ell}^k &\coloneqq \Big(2\big(\mathcal{J}_\ell^{k-1}(u_\ell^k) - \mathcal{J}_\ell^{*,k-1}(\boldsymbol{\sigma}_\ell^k) \big) \Big)^{\frac{1}{2}} \\ &\overset{(10.2a)}{=} \|(\boldsymbol{A}_\ell^{k-1})^{-\frac{1}{2}} (\boldsymbol{A}_\ell^{k-1} \nabla u_\ell^k - \boldsymbol{b}_\ell^{k-1} + \boldsymbol{\sigma}_\ell^k)\|. \end{aligned} \tag{5.2b}$$

5.2 Augmented energy difference and the associated estimator

Recalling the notation in (3.6b), as in (4.5d) but with the weight (3.7b), we define the iterative linearization estimator $\widehat{\eta}_{\mathrm{iter},\ell}^k$ by

$$\widehat{\eta}_{\mathrm{iter},\ell}^k \coloneqq \|(\boldsymbol{A}_\ell^{k-1})^{-\frac{1}{2}} (a_\ell^k \nabla u_\ell^k - \boldsymbol{\xi}_\ell^k)\|. \tag{5.3}$$

Observe that with the same reasoning as in Remark 4.3, if $(u_\ell^k)_{k\geq 1}$ converges in $H_0^1(\Omega)$, then we can have $\widehat{\eta}_{\mathrm{iter},\ell}^k$ as small as needed. Then, we define a computable weight $\lambda_\ell^k \geq 0$ from the estimators (4.1b) (using $\boldsymbol{\sigma}_\ell^k$ of (3.6) with the choice (3.7b)), (5.2b), and (5.3) by

$$\lambda_\ell^k \coloneqq \frac{\eta_{\mathrm{N},\ell}^k}{\eta_{\mathrm{L},\ell}^k + \widehat{\eta}_{\mathrm{iter},\ell}^k}. \tag{5.4}$$

Finally, we define the augmented energy difference $\mathcal{E}_\ell^k$ and estimator η_ℓ^k by

$$\mathcal{E}_\ell^k \coloneqq \frac{1}{2}\left(\mathcal{E}_{\mathrm{N},\ell}^k + \lambda_\ell^k \mathcal{E}_{\mathrm{L},\ell}^k \right) \quad \text{and} \quad \eta_\ell^k \coloneqq \frac{1}{2}\left(\eta_{\mathrm{N},\ell}^k + \lambda_\ell^k \eta_{\mathrm{L},\ell}^k \right). \tag{5.5}$$

Lemma 5.1 (Weight λ_ℓ^k)**.** *There holds*

$$\lambda_\ell^k \leq a_{\rm m}^{-\frac{1}{2}} A_{\rm c}^{\frac{1}{2}}. \tag{5.6}$$

Proof. See Section 9. □

Remark 5.2 (Weight λ_ℓ^k and uniform equivalence of η_ℓ^k and $\eta_{\mathrm{N},\ell}^k$)**.** *The weight λ_ℓ^k from (5.4) ensures a balance between the two components $\eta_{\mathrm{N},\ell}^k$ and $\lambda_\ell^k \eta_{\mathrm{L},\ell}^k$ in (5.5). In particular, $\lambda_\ell^k \eta_{\mathrm{L},\ell}^k = \eta_{\mathrm{N},\ell}^k$ in the limit $\widehat{\eta}_{\mathrm{iter},\ell}^k = 0$, whereby simply $\eta_\ell^k = \eta_{\mathrm{N},\ell}^k$. Moreover, from (5.4)–(5.5), at any linearization iteration $k \geq 1$,*

$$\frac{1}{2}\eta_{\mathrm{N},\ell}^k \leq \eta_\ell^k \leq \eta_{\mathrm{N},\ell}^k, \tag{5.7}$$

so that the augmented estimator η_ℓ^k of (5.5) is uniformly equivalent to the standard primal–dual gap estimator $\eta_{\mathrm{N},\ell}^k$ of (4.1b). This construction is well defined; in particular, the inclusion of the estimator $\widehat{\eta}_{\mathrm{iter},\ell}^k$ ensures that λ_ℓ^k is uniformly bounded for every $k \geq 1$ as per (5.6). This is in turn used in the error consistency of Lemma 5.3 and in Theorem 5.5 below.

Lemma 5.3 (Error consistency)**.** *Let the error $\mathcal{E}_\ell^k$ be given by (5.5). Then there holds*

$$\frac{1}{2}\mathcal{E}_{\mathrm{N},\ell}^k \leq \mathcal{E}_\ell^k \leq \frac{1}{2}\left(\mathcal{E}_{\mathrm{N},\ell}^k + a_{\rm m}^{-\frac{1}{2}} A_{\rm c}^{\frac{1}{2}} \mathcal{E}_{\mathrm{L},\ell}^k\right) \lesssim \mathcal{E}_{\mathrm{N},\ell}^k + \|\boldsymbol{\nabla}(u_\ell^k - u_\ell^{k-1})\|, \tag{5.8}$$

where the last inequality holds up to constants depending on $a_{\rm m}, a_{\rm c}, A_{\rm m}, A_{\rm c}$. In particular, $\mathcal{E}_\ell^k \to 0$ if and only if $u_\ell^k \to u$ in $H_0^1(\Omega)$.

Proof. See Section 9. □

Remark 5.4 (Augmented energy difference)**.** *From (5.7), the estimators $\eta_{\mathrm{N},\ell}^k$ and η_ℓ^k are uniformly equivalent. In that respect, Theorem 5.5 shows that the standard primal–dual gap estimator $\eta_{\mathrm{N},\ell}^k$ gives a guaranteed and potentially robust bound for the augmented energy difference $\mathcal{E}_\ell^k$ in place of the energy difference $\mathcal{E}_{\mathrm{N},\ell}^k$ of Theorem 4.4. As per (5.8), the modification of $\mathcal{E}_{\mathrm{N},\ell}^k$ to $\mathcal{E}_\ell^k$ is a bit more subtle in terms of the equivalence constant. In practice, though, we expect the situation to be better in that the added linearization component $\mathcal{E}_{\mathrm{L},\ell}^k$ multiplied by the weight λ_ℓ^k makes again $\mathcal{E}_\ell^k$ comparable in size to $\mathcal{E}_{\mathrm{N},\ell}^k$.*

5.3 Data oscillation and quadrature-type estimators

As in Section 4.3, let

$$(\widehat{\eta}_{\mathrm{osc},\ell}^k)^2 \coloneqq \sum_{K\in\mathcal{T}_\ell}\left[\frac{h_K}{\pi \inf_K (A_{\mathrm{m},\ell}^{k-1})^{\frac{1}{2}}}\|(I-\Pi_{\ell,p})f\|_K\right]^2, \tag{5.9a}$$

$$(\widehat{\eta}_{\mathrm{osc,q},\ell}^k)^2 \coloneqq \sum_{\boldsymbol{a}\in\mathcal{V}_\ell}(\widehat{\eta}_{\mathrm{osc,q},\ell}^{\boldsymbol{a},k})^2 \quad \text{and} \quad (\widehat{\eta}_{\mathrm{q},\ell}^k)^2 \coloneqq \sum_{\boldsymbol{a}\in\mathcal{V}_\ell}(\widehat{\eta}_{\mathrm{q},\ell}^{\boldsymbol{a},k})^2, \tag{5.9b}$$

where, for all vertices $\boldsymbol{a} \in \mathcal{V}_\ell$, recalling the notation from (3.6b),

$$(\widehat{\eta}_{\mathrm{osc,q},\ell}^{\boldsymbol{a},k})^2 \coloneqq \frac{1}{\inf_{\omega_\ell^{\boldsymbol{a}}} A_{\mathrm{m},\ell}^{k-1}}\sum_{K\in\mathcal{T}_\ell^{\boldsymbol{a}}}\left[\frac{h_K}{\pi}\|(I-\Pi_{\ell,p})\gamma_\ell^{\boldsymbol{a},k}\|_K\right]^2, \tag{5.9c}$$

$$\widehat{\eta}_{\mathrm{q},\ell}^{\boldsymbol{a},k} \coloneqq \|(\boldsymbol{A}_\ell^{k-1})^{-\frac{1}{2}}(\psi_\ell^{\boldsymbol{a}}(\boldsymbol{I}-\boldsymbol{\Pi}_{\ell,p-1}^{\boldsymbol{RTN}})\boldsymbol{\xi}_\ell^k)\|_{\omega_\ell^{\boldsymbol{a}}}. \tag{5.9d}$$

5.4 A posteriori estimate of the augmented energy difference

We now present our main result giving an a posteriori estimate based on the augmented energy difference and estimator defined in (5.5).

Theorem 5.5 (A posteriori estimate of the augmented energy difference)**.** *Suppose Assumption 2.1 and let u be the weak solution of (2.2). Let u_ℓ^k be its finite element approximation given by (2.6) on mesh $\mathcal{T}_\ell$, $\ell \geq 0$, and linearization step $k \geq 1$, for any iterative linearization satisfying Assumption 2.2. Let $\boldsymbol{\sigma}_\ell^k$ be* *the equilibrated flux defined by* (3.6) *with the choice* (3.7b)*. Let* $u^k_{\langle\ell\rangle}$ *be given by* (5.1)*, and the augmented error* $\mathcal{E}^k_\ell$ *and estimator* η^k_ℓ *by* (5.5)*. Then*

$$\mathcal{E}^k_\ell \le \eta^k_\ell + \eta^k_{\mathrm{osc},\ell} + \frac{\lambda^k_\ell}{2}\widehat{\eta}^k_{\mathrm{osc},\ell}, \tag{5.10a}$$

$$\eta^k_\ell \lesssim \widehat{C}^k_\ell \mathcal{E}^k_\ell + \lambda^k_\ell(\widehat{C}^k_\ell \widehat{\eta}^k_{\mathrm{q},\ell} + \widehat{\eta}^k_{\mathrm{osc,q},\ell} + \widehat{\eta}^k_{\mathrm{iter},\ell}), \tag{5.10b}$$

where the hidden constant only depends on the space dimension d*, the mesh shape-regularity* $\kappa_{\mathcal{T}}$*, and possibly, when* $d \ge 4$*, the polynomial degree* p*, with*

$$\widehat{C}^k_\ell := \max_{\boldsymbol{a}\in\mathcal{V}_\ell}\left(\frac{\sup_{\omega^{\boldsymbol{a}}_\ell} A^{k-1}_{\mathrm{c},\ell}}{\inf_{\omega^{\boldsymbol{a}}_\ell} A^{k-1}_{\mathrm{m},\ell}}\right)^{\frac12} \begin{cases} = 1 & \text{for the Zarantonello linearization,} \\ \le \left(\dfrac{A_{\mathrm{c}}}{A_{\mathrm{m}}}\right)^{\frac12} & \text{in general.}\end{cases} \tag{5.11}$$

Proof. See Section 10. □

Remark 5.6 (Robustness for the Zarantonello linearization)**.** *In the Zarantonello linearization of Example 2.5, since* $\widehat{C}^k_\ell = 1$*, we obtain via* (5.10) *an estimation of the augmented energy difference* $\mathcal{E}^k_\ell$ *by the estimator* η^k_ℓ *(under small oscillation, quadrature-type, and iterative linearization errors) whose quality is independent of the nonlinear function* a*. As we will see in the proof of Theorem 5.5, this relies on the fact that here* $\boldsymbol{A}^{k-1}_\ell = \gamma \boldsymbol{I}_d$*, the linearized problem* (5.1) *features a constant diffusion tensor, and consequently the associated error* (5.2a) *and estimator* (5.2b) *simplify respectively to* $\mathcal{E}^k_{\mathrm{L},\ell} = \gamma^{\frac12}\|\boldsymbol{\nabla}(u^k_\ell - u^k_{\langle\ell\rangle})\|$ *and* $\eta^k_{\mathrm{L},\ell} = \|\gamma^{-\frac12}(\gamma\boldsymbol{\nabla}u^k_\ell - \boldsymbol{b}^{k-1}_\ell + \boldsymbol{\sigma}^k_\ell)\|$*.*

Remark 5.7 (Robustness in the general case)**.** *The constant* $\widehat{C}^k_\ell$ *can be easily calculated in practice, without knowing the continuous solution* u *of* (2.2)*. It is in particular defined from merely patchwise variations of the linearization matrix* $\boldsymbol{A}^{k-1}_\ell$ *(recall* (2.8)*). For the Picard and damped Newton iteration cases of Examples 2.4 and 2.6, in particular, the local ratio of the functions* $A^{k-1}_{\mathrm{c},\ell}$ *and* $A^{k-1}_{\mathrm{m},\ell}$ *is a lower bound for that of the global constants* A_{c} *and* A_{m} *given in* (2.8c)*, typically bringing* $\widehat{C}^k_\ell$ *close to 1 as in the Zarantonello case. This is indeed observed in the numerical experiments of Section 6. Importantly,* $\widehat{C}^k_\ell$ *allows us to quantify the quality of the estimates in any situation: whenever it is small, we can affirm robustness a posteriori.*

Remark 5.8 (Theorem 5.5 at the convergence of iterative linearization / impact of the chosen iterative linearization)**.** *Suppose that* $u^k_\ell \to u_\ell$ *in* $H^1_0(\Omega)$*, i.e., the solution* u^k_ℓ *of the iterative linearization* (2.6) *converges to the solution* u_ℓ *of the discrete nonlinear problem* (2.5a)*. In the limit,* $\widehat{\eta}^k_{\mathrm{iter},\ell}$ *from* (5.3) *vanishes and all the different iterative linearizations, cf. the examples of Section 2.3.2, yield the unique finite element approximation* u_ℓ*. Nevertheless, in Theorem 5.5, the augmented energy difference* $\mathcal{E}^k_\ell$ *from* (5.5) *is still (possibly) influenced by the chosen iterative linearization, in particular by the (limit) values of* $\boldsymbol{A}^{k-1}_\ell$ *and* $\boldsymbol{b}^{k-1}_\ell$ *as per* (5.2)*, cf. also Remarks 5.2 and 5.3.*

6 Numerical results

In this section, we present numerical experiments that serve to illustrate Theorems 4.4 and 5.5. Thus, we will primarily be interested in the effectivity indices

$$I^k_{\mathrm{N},\ell} := \frac{\eta^k_{\mathrm{N},\ell}}{\mathcal{E}^k_{\mathrm{N},\ell}}, \quad I^k_\ell := \frac{\eta^k_\ell}{\mathcal{E}^k_\ell}, \quad I^k_{\mathrm{L},\ell} := \frac{\eta^k_{\mathrm{L},\ell}}{\mathcal{E}^k_{\mathrm{L},\ell}}, \tag{6.1}$$

where the last one brings insight into the augmentation of Section 5.1. In particular, our numerical experiments study the robustness of our estimates with respect to the ratio $a_{\mathrm{c}}/a_{\mathrm{m}}$ from (2.1) where we consider $a_{\mathrm{c}}/a_{\mathrm{m}} = 10^i$, $i \in \{0,\dots,7\}$. We present results for the three linearization methods of Examples 2.4, 2.5, and 2.6 after the convergence criterion

$$\|\boldsymbol{\nabla}(u^{\overline{k}-1}_\ell - u^{\overline{k}}_\ell)\| < 10^{-6} \tag{6.2}$$

has been reached.

In addition to V_ℓ^p as defined in Section 2.2, we also consider a richer discrete space $V_{\tilde\ell}^{\tilde p}$ obtained by refining the mesh $\mathcal{T}_\ell$ and using higher-order polynomials, $\ell < \tilde\ell$ and $p < \tilde p$. This space serves as an approximation to $H_0^1(\Omega)$, so that we can approximately compute $u_{\langle\ell\rangle}^k$ defined in (5.1b) at each iteration k of the linearization method. This only serves here for the evaluation of the error $\mathcal{E}_{\mathrm{L},\ell}^k$; it is not needed to evaluate our estimators $\eta_{\mathrm{N},\ell}^k$, $\eta_{\mathrm{L},\ell}^k$, and η_ℓ^k.

For all examples, we use the method of manufactured solutions, i.e. we choose a solution u and construct f through (1.1). The boundary conditions are then enforced by the true solution. All experiments were conducted using the `Gridap.jl` finite element software package [1, 43].

6.1 Smooth solution

We consider a unit square domain $\Omega = (0,1)^2$. We set for all $(x,y) \in \Omega$,

$$u(x,y) \coloneqq 10\, x(x-1)y(y-1). \tag{6.3}$$

For the space V_ℓ^p, we use a polynomial degree $p = 1$ and a uniform triangular mesh consisting of 8192 elements for a total of 3969 DOFs. We consider three different nonlinear functions $a : [0,\infty) \to (0,\infty)$ (independent of the spatial coordinate $\boldsymbol{x} \in \Omega$) satisfying Assumption 2.1. We first consider the following example, in which the function a is monotone (decreasing).

Example 6.1 (Mean curvature nonlinearity)**.** *The mean curvature nonlinearity (cf. [14]) is defined such that for all $r \in [0,\infty)$,*

$$a(r) \coloneqq a_{\mathrm{m}} + \frac{a_{\mathrm{c}} - a_{\mathrm{m}}}{\sqrt{1+r^2}}, \tag{6.4}$$

where $a_{\mathrm{m}}, a_{\mathrm{c}} \in (0,\infty)$ with $a_{\mathrm{m}} \le a_{\mathrm{c}}$. Observe that Assumption 2.1 holds for the mean curvature nonlinearity. Indeed, we use Proposition A.2 observing that, for all $r \in [0,\infty)$,

$$\phi''(r) = a_{\mathrm{m}} + \frac{a_{\mathrm{c}} - a_{\mathrm{m}}}{(1+r^2)^{\frac{3}{2}}} \in [a_{\mathrm{m}}, a_{\mathrm{c}}].$$

The results for the effectivity indices (6.1) are presented in Figure 2, taking $a_{\mathrm{m}} = 1$. We see that they vary only very mildly with respect to the ratio $a_{\mathrm{m}}/a_{\mathrm{c}}$ and that all values are below 1.2. This illustrates the robustness for the Zarantonello linearization that has been proven in Theorem 5.5. For the Newton and Picard linearizations, we also compute and display the constant $\widehat{C}_\ell^{\overline{k}}$ of (5.11). Since we see that $\widehat{C}_\ell^{\overline{k}}$ is uniformly close to 1 (bounded by 3), we are sure that the effectivity index I_ℓ^k will be small and uniformly bounded even prior to computing it. This is the meaning of "affirm robustness a posteriori" of Remark 5.7.

We now consider the following nonmonotone nonlinear function a similar to the example given in [31, Section 5.3.2].

Example 6.2 (Exponential nonlinearity)**.** *The exponential nonlinearity is defined such that for all $r \in [0,\infty)$,*

$$a(r) \coloneqq a_{\mathrm{m}} + (a_{\mathrm{c}} - a_{\mathrm{m}})\frac{1 - e^{-\frac{3}{2}r^2}}{1 + 2e^{-\frac{3}{2}}}, \tag{6.5}$$

where again $a_{\mathrm{m}}, a_{\mathrm{c}} \in (0,\infty)$ with $a_{\mathrm{m}} \le a_{\mathrm{c}}$. Observe that Assumption 2.1 holds for the exponential nonlinearity. Indeed, we again use Proposition A.2 observing that, for all $r \in [0,\infty)$,

$$\phi''(r) = a_{\mathrm{m}} + (a_{\mathrm{c}} - a_{\mathrm{m}})\frac{1 + (3r^2-1)e^{-\frac{3}{2}r^2}}{1 + 2e^{-\frac{3}{2}}} \in [a_{\mathrm{m}}, a_{\mathrm{c}}].$$

The results, again with $a_{\mathrm{m}} = 1$, are presented in Figure 3. The Picard linearization is not included because the solver does not converge for large values of the ratio $a_{\mathrm{c}}/a_{\mathrm{m}}$. We observe that the results for the Zarantonello iteration are similar to those of Figure 2. However, the effectivity indices of the Newton iteration seem to start to deteriorate for large values of the ratio $a_{\mathrm{c}}/a_{\mathrm{m}}$. We can see that the reason is that the constant $\widehat{C}_\ell^{\overline{k}}$ is becoming very large. This constant is thus here a good indicator that the robustness may not be obtained; in this case, we cannot "affirm robustness a posteriori" and it indeed seems not to hold. For this example, we also present, in Figure 4, the component errors $\mathcal{E}_{\mathrm{N},\ell}^{\overline{k}}$ and $\lambda_\ell^{\overline{k}}\mathcal{E}_{\mathrm{L},\ell}^{\overline{k}}$, as well as the factor $\lambda_\ell^{\overline{k}}$, see (5.4)–(5.5). We observe that $\mathcal{E}_{\mathrm{N},\ell}^{\overline{k}}$ and $\lambda_\ell^{\overline{k}}\mathcal{E}_{\mathrm{L},\ell}^{\overline{k}}$ stay very close, independently of the ratio $a_{\mathrm{c}}/a_{\mathrm{m}}$, which was our design. Remark, though, that $\lambda_\ell^{\overline{k}} \simeq 1$ for Newton, whereas $\lambda_\ell^{\overline{k}} \simeq (a_{\mathrm{c}}/a_{\mathrm{m}})^{\frac{1}{2}}$ for Zarantonello.

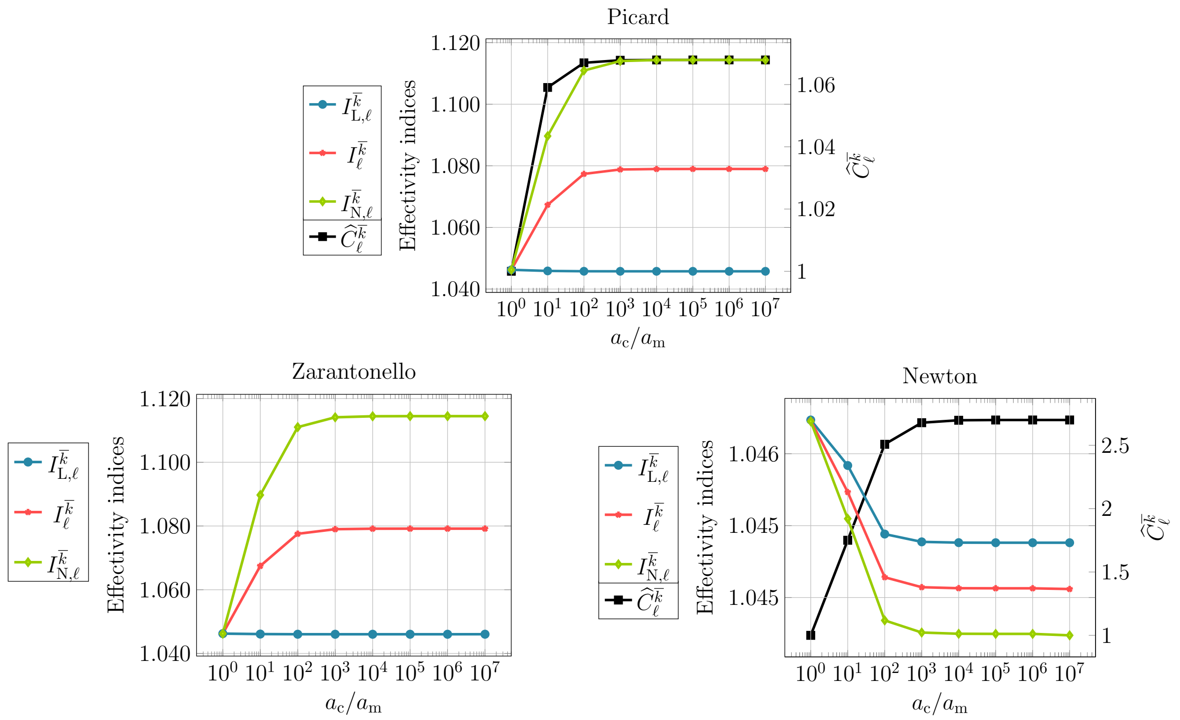

Figure 2: [Mean curvature nonlinearity (6.4), smooth solution (6.3), unit square domain, 3969 DOFs] Effectivity indices from (6.1) and the computable constant $\widehat{C}_\ell^{\bar{k}}$ from (5.11).

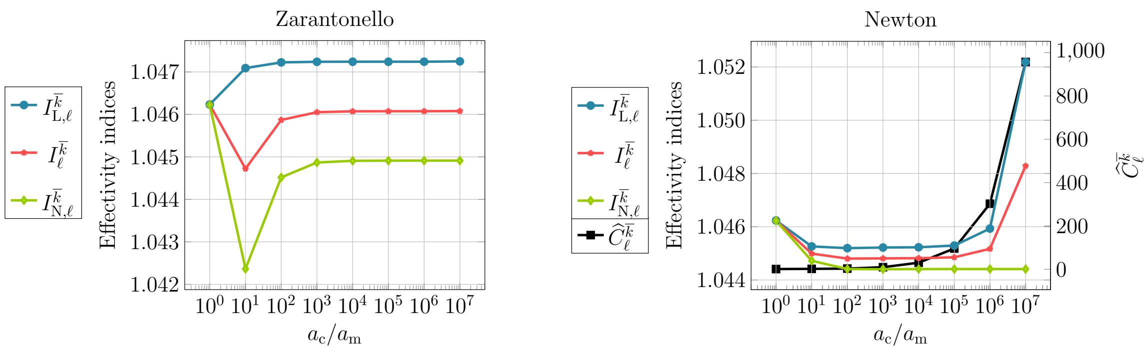

Figure 3: [Exponential nonlinearity (6.5), smooth solution (6.3), unit square domain, 3969 DOFs] Effectivity indices from (6.1) and the computable constant $\widehat{C}_\ell^{\bar{k}}$ from (5.11).

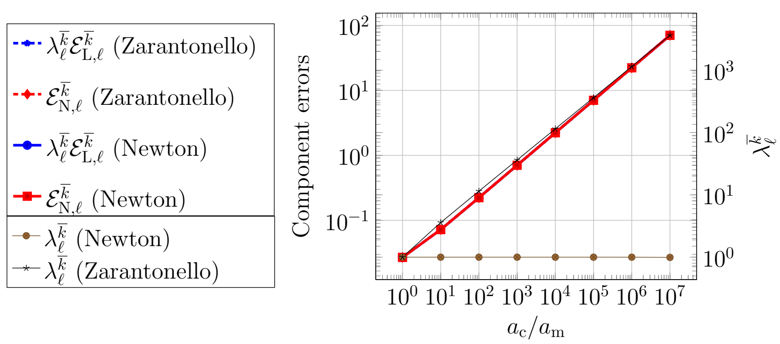

Figure 4: [Exponential nonlinearity (6.5), smooth solution (6.3), unit square domain, 3969 DOFs] Components $\mathcal{E}_{\mathrm{N},\ell}^{\bar{k}}$ and $\lambda_\ell^{\bar{k}}\mathcal{E}_{\mathrm{L},\ell}^{\bar{k}}$ from (5.5) together with the weight $\lambda_\ell^{\bar{k}}$ from (5.4).

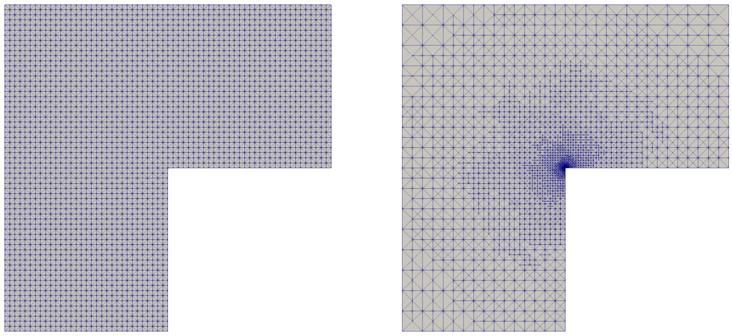

(a) 2945 DOFs (b) 2417 DOFs

Figure 5: Uniformly (left) and adaptively (right) refined meshes for the L-shaped domain with the singular solution (6.6). The adaptive mesh corresponds to the 28th iteration of Algorithm 6.3.

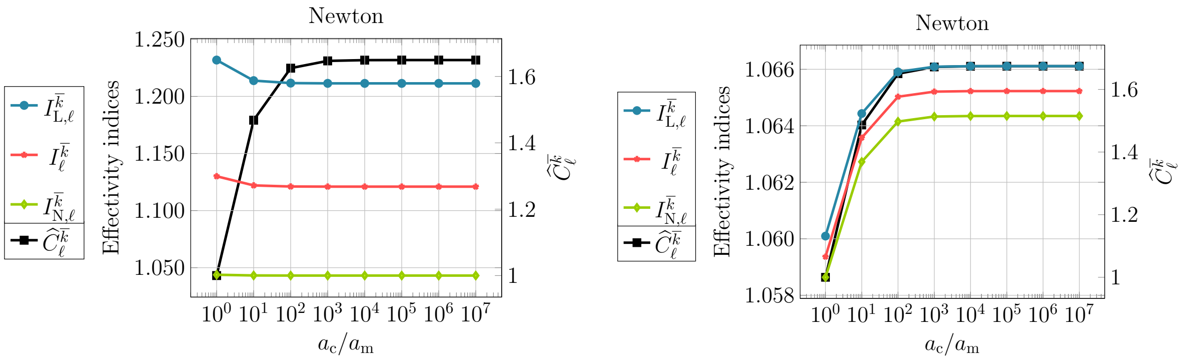

Figure 6: [Exponential nonlinearity (6.5), singular solution (6.6), L-shaped domain] Effectivity indices from (6.1) and the computable constant $\widehat{C}^{\overline{k}}_{\ell}$ from (5.11), for the uniform mesh (left) and the adaptive mesh (right) shown in Figure 5.

6.2 Singular solution

We consider the L-shaped domain $\Omega = (-1,1)^2 \setminus ([0,1) \times (-1,0])$ and the singular solution u in polar coordinates $(\rho,\theta) \in [0,\infty) \times [0,2\pi)$

$$u(\rho,\theta) = \rho^{\alpha} \sin(\alpha\theta) \tag{6.6}$$

with $\alpha \coloneqq \frac{2}{3}$, so that $u \in H^{1+\frac{2}{3}-\varepsilon}(\Omega)$ for all $\varepsilon > 0$. We consider the exponential nonlinearity of Example 6.2 again with $a_{\mathrm{m}} = 1$; this choice of solution ensures that the right-hand side f belongs to $L^2(\Omega)$ despite the singularity in the norm of the gradient for the L-shaped solution (6.6).

We consider two different meshes to analyze the results, see Figure 5. One mesh is obtained by taking an initial uniform triangulation of Ω, while the other one is adaptive following Algorithm 6.3.

The results are presented in Figure 6. The Newton iteration showcases, for both meshes, effectivity indices close to 1, which stabilize for large enough values of the ratio $a_{\mathrm{m}}/a_{\mathrm{c}}$. Moreover, the effectivity indices corresponding to the adaptive meshes are closer to 1 than those corresponding to the uniform meshes. Since $\widehat{C}^{\overline{k}}_{\ell}$ takes small values below 2, we can again claim robustness a posteriori, see Remark 5.7.

6.3 Convergence on a sequence of adaptively refined meshes

Due to the singularity in the solution of the previous section, it is of interest to consider a local adaptive mesh refinement strategy. We thus need to compute the contribution of the estimator $\eta^k_{\mathrm{N},\ell}$ to each mesh element which is nonnegative. In order to do that, cf. the discussion in, e.g., [4, Proposition 4.9], we use (2.3), (3.1), and (3.9) to rewrite the estimator $\eta_{\mathrm{N},\ell}^k$ of (4.1b) as

$$\eta_{\mathrm{N},\ell}^k = \left(2\int_\Omega \left(\phi^*(\cdot,|\boldsymbol{\sigma}_\ell^k|) + \phi(\cdot,|\boldsymbol{\nabla} u_\ell^k|) + \boldsymbol{\sigma}_\ell^k\cdot\boldsymbol{\nabla} u_\ell^k\right)\right)^{\frac{1}{2}} = \left(\sum_{K\in\mathcal{T}_\ell}(\eta_{\mathrm{N},K}^k)^2\right)^{\frac{1}{2}}, \tag{6.7a}$$

$$(\eta_{\mathrm{N},K}^k)^2 \coloneqq 2\int_K \left(\phi^*(\cdot,|\boldsymbol{\sigma}_\ell^k|) + \phi(\cdot,|\boldsymbol{\nabla} u_\ell^k|) + \boldsymbol{\sigma}_\ell^k\cdot\boldsymbol{\nabla} u_\ell^k\right), \quad K\in\mathcal{T}_\ell. \tag{6.7b}$$

Here, recalling the generalized Young inequality, cf. [32],

$$\phi(\cdot,|\boldsymbol{x}|) + \phi^*(\cdot,|\boldsymbol{y}|) + \boldsymbol{x}\cdot\boldsymbol{y} \geq 0 \qquad \forall \boldsymbol{x},\boldsymbol{y}\in\mathbb{R}^d, \tag{6.8}$$

it follows that for all $K\in\mathcal{T}_\ell$, indeed $\eta_{\mathrm{N},K}^k \geq 0$. We then use the standard newest vertex bisection algorithm, see [9] and the references therein, as follows.

Algorithm 6.3 (Adaptive refinement)**.** *Let $\varepsilon_{\mathrm{STOP}}$ and $\theta\in(0,1)$ be parameters, and let $\mathcal{T}_0$ be a conforming initial triangulation of Ω. Let $u_0^0\in V_0^1$ be an initial linearization guess. For $\ell\geq 0$:*

1. ***Solve**: Starting from u_ℓ^0, solve the linearized problems (2.6) until the convergence criterion (6.2) is satisfied.*
2. ***Estimate**: Compute the elementwise estimators $(\eta_{\mathrm{N},K}^{\overline{k}})_{K\in\mathcal{T}_\ell}$ of (6.7b).*
   If $\eta_{\mathrm{N},\ell}^{\overline{k}} < \varepsilon_{\mathrm{STOP}}$, then stop.
3. ***Mark**: Choose a set $\mathcal{M}_\ell\subset\mathcal{T}_\ell$ with minimal cardinality such that*

$$\sum_{K\in\mathcal{M}_\ell}(\eta_{\mathrm{N},K}^{\overline{k}})^2 \geq \theta^2\sum_{K\in\mathcal{T}_\ell}(\eta_{\mathrm{N},K}^{\overline{k}})^2. \tag{6.9}$$

4. ***Refine**: Perform the newest vertex bisection on the set $\mathcal{M}_\ell$. Set $\ell\coloneqq\ell+1$, $u_\ell^0\coloneqq u_{\ell-1}^{\overline{k}}$, and go to step 1.*

The results of the refinement study are displayed in Figure 7, for the exponential nonlinearity (6.5) and the singular solution (6.6). We consider two values of the parameter $a_{\mathrm{c}}/a_{\mathrm{m}}$, namely 10^3 and 10^6. We note that for both values of the ratio, the asymptotic rates for the estimator and error agree with the theoretical optimal rate of $(\mathrm{DOFs})^{-1/2}$ for the adaptive algorithm; we observe no distinguishable difference in this graphic representation between $a_{\mathrm{c}}/a_{\mathrm{m}} = 10^3$ and 10^6.

We also made an analogous study on the augmented error $\mathcal{E}_\ell^{\overline{k}}$ and the estimator $\eta_\ell^{\overline{k}}$, with the same strategy of refinement, using the local version $\eta_K^{\overline{k}} \coloneqq \eta_{\mathrm{N},K}^{\overline{k}} + \lambda_\ell^{\overline{k}}\eta_{\mathrm{L},K}^{\overline{k}}$, for all $K\in\mathcal{T}_\ell$, of the estimator $\eta_\ell^{\overline{k}}$. The results are displayed in Figure 8. We observe a similar behavior of the asymptotic rates as in Figure 7.

In conclusion, the adaptive mesh refinement is more efficient than the uniform mesh refinement since it requires a smaller number of DOFs for the same precision. The behavior seems to be independent of the strength of the nonlinearity $a_{\mathrm{c}}/a_{\mathrm{m}}$.

7 Proof of Lemma 4.1

Proof of Lemma 4.1. Observing that by integration by parts (IBP), $\frac{\partial}{\partial r}((|\boldsymbol{\sigma}_\ell^k| - r)\phi^{*\prime}(\cdot,r)) = (|\boldsymbol{\sigma}_\ell^k| - r)\phi^{*\prime\prime}(\cdot,r) - \phi^{*\prime}(\cdot,r)$, we obtain, a.e. in Ω,

$$\begin{aligned}\phi^*(\cdot,|\boldsymbol{\sigma}_\ell^k|) - \phi^*(\cdot,a_\ell^k|\boldsymbol{\nabla} u_\ell^k|) &= \int_{a_\ell^k|\boldsymbol{\nabla} u_\ell^k|}^{|\boldsymbol{\sigma}_\ell^k|}\phi^{*\prime}(\cdot,r)\,\mathrm{d}r\\ &\overset{\text{(IBP)}}{=} \int_{a_\ell^k|\boldsymbol{\nabla} u_\ell^k|}^{|\boldsymbol{\sigma}_\ell^k|}(|\boldsymbol{\sigma}_\ell^k| - r)\phi^{*\prime\prime}(\cdot,r)\,\mathrm{d}r - \Big[(|\boldsymbol{\sigma}_\ell^k| - r)\phi^{*\prime}(\cdot,r)\Big]_{a_\ell^k|\boldsymbol{\nabla} u_\ell^k|}^{|\boldsymbol{\sigma}_\ell^k|}\\ &\overset{(3.3)}{=} \int_{a_\ell^k|\boldsymbol{\nabla} u_\ell^k|}^{|\boldsymbol{\sigma}_\ell^k|}\frac{|\boldsymbol{\sigma}_\ell^k| - r}{\phi''(\cdot,\phi'^{-1}(\cdot,r))}\,\mathrm{d}r + (|\boldsymbol{\sigma}_\ell^k| - a_\ell^k|\boldsymbol{\nabla} u_\ell^k|)|\boldsymbol{\nabla} u_\ell^k|,\end{aligned} \tag{7.1}$$

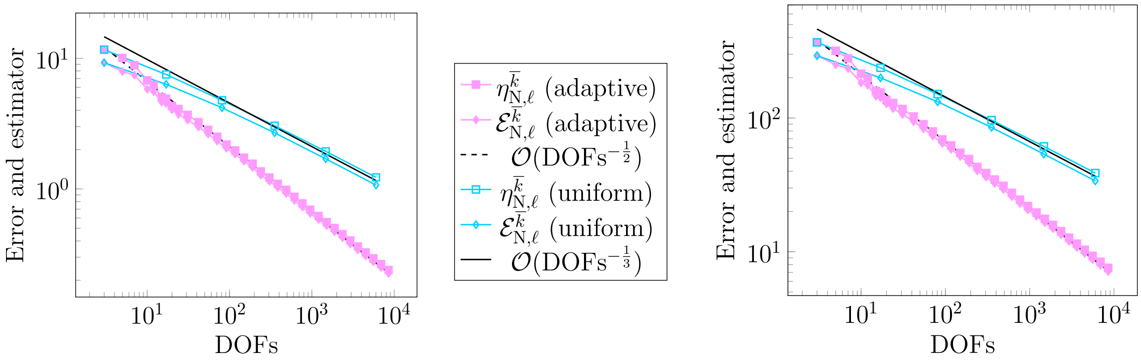

Figure 7: [Exponential nonlinearity (6.5), singular solution (6.6), L-shaped domain, uniform vs adaptive mesh refinement] Convergence rates of $\mathcal{E}_{\mathrm{N},\ell}^{\overline{k}}$ and $\eta_{\mathrm{N},\ell}^{\overline{k}}$ for uniform and adaptive mesh refinement for $a_{\mathrm{c}}/a_{\mathrm{m}}$ equal to 10^3 (left) and 10^6 (right).

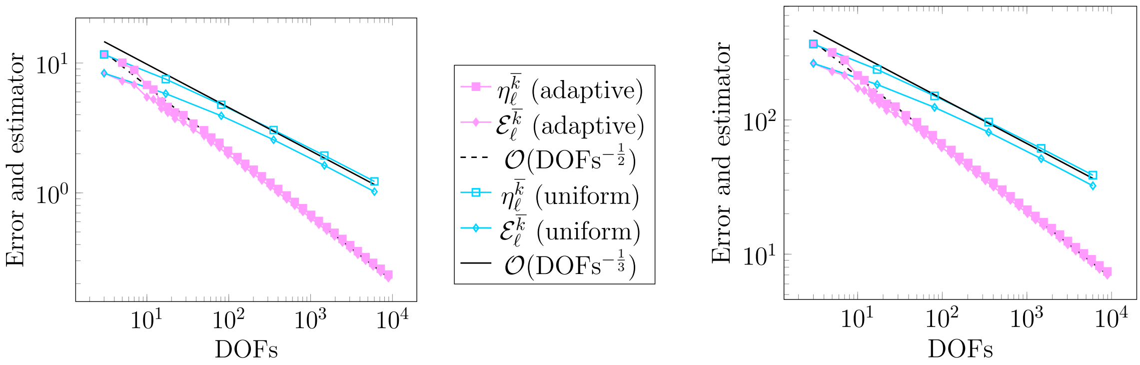

Figure 8: [Exponential nonlinearity (6.5), singular solution (6.6), L-shaped domain, uniform vs adaptive mesh refinement] Convergence rates of $\mathcal{E}_{\ell}^{\overline{k}}$ and $\eta_{\ell}^{\overline{k}}$ for uniform and adaptive mesh refinement for $a_{\mathrm{c}}/a_{\mathrm{m}}$ equal to 10^3 (left) and 10^6 (right).

where we used the fact that $\phi'^{-1}(\cdot, a_\ell^k|\boldsymbol{\nabla} u_\ell^k|) = \phi'^{-1}(\cdot, \phi'(\cdot, |\boldsymbol{\nabla} u_\ell^k|)) = |\boldsymbol{\nabla} u_\ell^k|$ thanks to (A.2). Reusing this relation together with the definitions (2.3) of $\mathcal{J}$ and (3.1) of $\mathcal{J}^*$, we obtain the right-hand side of (4.4b) by writing

$$
\begin{aligned}
(\eta_{\mathrm{N},\ell}^k)^2 &\overset{(4.1b)}{=} 2\int_\Omega \left(\phi^*(\cdot, |\boldsymbol{\sigma}_\ell^k|) + \phi(\cdot, |\boldsymbol{\nabla} u_\ell^k|)\right) - (f, u_\ell^k) \\
&\overset{(3.9)}{=} 2\int_\Omega \left(\phi^*(\cdot, |\boldsymbol{\sigma}_\ell^k|) + \phi(\cdot, |\boldsymbol{\nabla} u_\ell^k|) + \boldsymbol{\sigma}_\ell^k \cdot \boldsymbol{\nabla} u_\ell^k\right) \\
&\overset{(3.2b)}{=} 2\int_\Omega \left(\phi^*(\cdot, |\boldsymbol{\sigma}_\ell^k|) - \phi^*(\cdot, a_\ell^k|\boldsymbol{\nabla} u_\ell^k|) + a_\ell^k|\boldsymbol{\nabla} u_\ell^k|^2 + \boldsymbol{\sigma}_\ell^k \cdot \boldsymbol{\nabla} u_\ell^k\right) \\
&\overset{(7.1)}{=} 2\int_\Omega \left[\int_{a_\ell^k|\boldsymbol{\nabla} u_\ell^k|}^{|\boldsymbol{\sigma}_\ell^k|} \frac{|\boldsymbol{\sigma}_\ell^k| - r}{\phi''(\cdot, \phi'^{-1}(\cdot, r))}\,\mathrm{d}r + \frac{1}{a_\ell^k}(|\boldsymbol{\sigma}_\ell^k||a_\ell^k \boldsymbol{\nabla} u_\ell^k| + \boldsymbol{\sigma}_\ell^k \cdot (a_\ell^k \boldsymbol{\nabla} u_\ell^k))\right] \\
&\overset{(4.3c)}{\leq} \int_\Omega \frac{2}{a_{\mathrm{m},\ell}^{\boldsymbol{\sigma},k}} \left(\left[-\frac{1}{2}(|\boldsymbol{\sigma}_\ell^k| - r)^2\right]_{a_\ell^k|\boldsymbol{\nabla} u_\ell^k|}^{|\boldsymbol{\sigma}_\ell^k|} + |\boldsymbol{\sigma}_\ell^k||a_\ell^k \boldsymbol{\nabla} u_\ell^k| + \boldsymbol{\sigma}_\ell^k \cdot (a_\ell^k \boldsymbol{\nabla} u_\ell^k)\right) \\
&= \int_\Omega \frac{1}{a_{\mathrm{m},\ell}^{\boldsymbol{\sigma},k}} \left[(|\boldsymbol{\sigma}_\ell^k| - a_\ell^k|\boldsymbol{\nabla} u_\ell^k|)^2 + 2(|\boldsymbol{\sigma}_\ell^k||a_\ell^k \boldsymbol{\nabla} u_\ell^k| + \boldsymbol{\sigma}_\ell^k \cdot (a_\ell^k \boldsymbol{\nabla} u_\ell^k))\right] \\
&\overset{(A.4a)}{=} \int_\Omega \frac{1}{a_{\mathrm{m},\ell}^{\boldsymbol{\sigma},k}} |a_\ell^k \boldsymbol{\nabla} u_\ell^k + \boldsymbol{\sigma}_\ell^k|^2,
\end{aligned}
\tag{7.2}
$$

where, in using (3.2b), we have set $s = a_\ell^k|\boldsymbol{\nabla} u_\ell^k|$, and where we used (4.3c) noticing that $|\boldsymbol{\sigma}_\ell^k||a_\ell^k \boldsymbol{\nabla} u_\ell^k| + \boldsymbol{\sigma}_\ell^k \cdot (a_\ell^k \boldsymbol{\nabla} u_\ell^k) \geq 0$ thanks to the Cauchy–Schwarz inequality, together with the fact that $|\boldsymbol{\sigma}_\ell^k| - r$ is of the same sign as $|\boldsymbol{\sigma}_\ell^k| - a_\ell^k|\boldsymbol{\nabla} u_\ell^k|$ for all $r \in (a_\ell^k|\boldsymbol{\nabla} u_\ell^k|, |\boldsymbol{\sigma}_\ell^k|)$. The left-hand side of (4.4b) is obtained with the same reasoning.

Now, observing that $\frac{\partial}{\partial r}((|\boldsymbol{\nabla} u_\ell^k| - r)\phi'(\cdot, r)) = (|\boldsymbol{\nabla} u_\ell^k| - r)\phi''(\cdot, r) - \phi'(\cdot, r)$ by integration by parts (IBP), we get

$$
\begin{aligned}
(\mathcal{E}_{\mathrm{N},\ell}^k)^2 &\overset{(4.1a),(2.3)}{=} 2\int_\Omega (\phi(\cdot, |\boldsymbol{\nabla} u_\ell^k|) - \phi(\cdot, |\boldsymbol{\nabla} u|)) - 2(f, u_\ell^k - u) \\
&\overset{(2.2a)}{=} 2\int_\Omega \int_{|\boldsymbol{\nabla} u|}^{|\boldsymbol{\nabla} u_\ell^k|} \phi'(\cdot, r)\,\mathrm{d}r - 2(a_u \boldsymbol{\nabla} u, \boldsymbol{\nabla}(u_\ell^k - u)) \\
&\overset{(\mathrm{IBP})}{=} 2\int_\Omega \left(\int_{|\boldsymbol{\nabla} u|}^{|\boldsymbol{\nabla} u_\ell^k|} (|\boldsymbol{\nabla} u_\ell^k| - r)\phi''(\cdot, r)\,\mathrm{d}r - \Big[(|\boldsymbol{\nabla} u_\ell^k| - r)\phi'(\cdot, r) \Big]_{|\boldsymbol{\nabla} u|}^{|\boldsymbol{\nabla} u_\ell^k|} \right) \\
&\qquad - 2(a_u \boldsymbol{\nabla} u, \boldsymbol{\nabla}(u_\ell^k - u)) \\
&\overset{(A.2)}{=} 2\int_\Omega \left(\int_{|\boldsymbol{\nabla} u|}^{|\boldsymbol{\nabla} u_\ell^k|} (|\boldsymbol{\nabla} u_\ell^k| - r)\phi''(\cdot, r)\,\mathrm{d}r + a_u(|\boldsymbol{\nabla} u_\ell^k||\boldsymbol{\nabla} u| - \boldsymbol{\nabla} u_\ell^k \cdot \boldsymbol{\nabla} u) \right).
\end{aligned}
\tag{7.3}
$$

From there, with the same reasoning as for (4.4b), we obtain the right-hand side of (4.4a), by writing

$$
\begin{aligned}
(\mathcal{E}_{\mathrm{N},\ell}^k)^2 &\overset{(7.3),(4.3c)}{\le} \int_\Omega a_{\mathrm{c},\ell}^{u,k} \left((|\boldsymbol{\nabla} u_\ell^k| - |\boldsymbol{\nabla} u|)^2 + 2(|\boldsymbol{\nabla} u_\ell^k||\boldsymbol{\nabla} u| - \boldsymbol{\nabla} u_\ell^k \cdot \boldsymbol{\nabla} u) \right) \\
&\overset{(A.4a)}{=} \int_\Omega a_{\mathrm{c},\ell}^{u,k} |\boldsymbol{\nabla} u_\ell^k - \boldsymbol{\nabla} u|^2.
\end{aligned}
\tag{7.4}
$$

The left-hand side of (4.4a) is obtained with the same reasoning. Moreover, since ϕ' is nondecreasing and $|\boldsymbol{\nabla} u_\ell^k| - r$ is of the same sign as $|\boldsymbol{\nabla} u_\ell^k| - |\boldsymbol{\nabla} u|$ for all $r \in (|\boldsymbol{\nabla} u|, |\boldsymbol{\nabla} u_\ell^k|)$, using the mean value inequality, we have a.e. in Ω,

$$
\begin{aligned}
\int_{|\boldsymbol{\nabla} u|}^{|\boldsymbol{\nabla} u_\ell^k|} (|\boldsymbol{\nabla} u_\ell^k| - r)\phi''(\cdot, r)\,\mathrm{d}r &\ge \int_{|\boldsymbol{\nabla} u|}^{|\boldsymbol{\nabla} u_\ell^k|} \frac{\phi'(\cdot, |\boldsymbol{\nabla} u_\ell^k|) - \phi'(\cdot, r)}{\operatorname*{ess\,sup}_{s \in (r, |\boldsymbol{\nabla} u_\ell^k|)} \phi''(\cdot, s)} \phi''(\cdot, r)\,\mathrm{d}r \\
&\overset{(4.3c)}{\ge} \frac{1}{a_{\mathrm{c},\ell}^{\boldsymbol{\nabla} u,k}} \int_{|\boldsymbol{\nabla} u|}^{|\boldsymbol{\nabla} u_\ell^k|} (\phi'(\cdot, |\boldsymbol{\nabla} u_\ell^k|) - \phi'(\cdot, r))\phi''(\cdot, r)\,\mathrm{d}r \\
&= \frac{1}{a_{\mathrm{c},\ell}^{\boldsymbol{\nabla} u,k}} \left[\phi'(\cdot, |\boldsymbol{\nabla} u_\ell^k|)\phi'(\cdot, r) - \frac{1}{2}\phi'(\cdot, r)^2 \right]_{|\boldsymbol{\nabla} u|}^{|\boldsymbol{\nabla} u_\ell^k|} \\
&\overset{(A.2)}{=} \frac{1}{a_{\mathrm{c},\ell}^{\boldsymbol{\nabla} u,k}} \left(\frac{1}{2}\left(|a_\ell^k \boldsymbol{\nabla} u_\ell^k|^2 + |a_u \boldsymbol{\nabla} u|^2 \right) - a_\ell^k a_u |\boldsymbol{\nabla} u_\ell^k||\boldsymbol{\nabla} u| \right),
\end{aligned}
\tag{7.5}
$$

where we used (4.3c) knowing that $|a_u \boldsymbol{\nabla} u| = \phi'(\cdot, |\boldsymbol{\nabla} u|)$ and $|a_\ell^k \boldsymbol{\nabla} u_\ell^k| = \phi'(\cdot, |\boldsymbol{\nabla} u_\ell^k|)$. Thus, observing that $|\boldsymbol{\nabla} u_\ell^k||\boldsymbol{\nabla} u| - \boldsymbol{\nabla} u_\ell^k \cdot \boldsymbol{\nabla} u \ge 0$ thanks to the Cauchy–Schwarz inequality, we obtain the left-hand side of (4.4c) by writing

$$
\begin{aligned}
(\mathcal{E}_{\mathrm{N},\ell}^k)^2 &\overset{(7.3),(7.5),(4.3c)}{\ge} \int_\Omega \frac{2}{a_{\mathrm{c},\ell}^{\boldsymbol{\nabla} u,k}} \left(\frac{1}{2}\left(|a_\ell^k \boldsymbol{\nabla} u_\ell^k|^2 + |a_u \boldsymbol{\nabla} u|^2 \right) - (a_\ell^k \boldsymbol{\nabla} u_\ell^k) \cdot (a_u \boldsymbol{\nabla} u) \right) \\
&= \int_\Omega \frac{1}{a_{\mathrm{c},\ell}^{\boldsymbol{\nabla} u,k}} |a_\ell^k \boldsymbol{\nabla} u_\ell^k - a_u \boldsymbol{\nabla} u|^2.
\end{aligned}
\tag{7.6}
$$

Finally, since $|\boldsymbol{\nabla} u_\ell^k| - r$ is of the same sign as $|\boldsymbol{\nabla} u_\ell^k| - |\boldsymbol{\nabla} u|$ for all $r \in (|\boldsymbol{\nabla} u|, |\boldsymbol{\nabla} u_\ell^k|)$, we have

$$
\begin{aligned}
\int_{|\boldsymbol{\nabla} u|}^{|\boldsymbol{\nabla} u_\ell^k|} (|\boldsymbol{\nabla} u_\ell^k| - r)\phi''(\cdot, r)\,\mathrm{d}r &\le (|\boldsymbol{\nabla} u_\ell^k| - |\boldsymbol{\nabla} u|) \int_{|\boldsymbol{\nabla} u|}^{|\boldsymbol{\nabla} u_\ell^k|} \phi''(\cdot, r)\,\mathrm{d}r \\
&\overset{(4.3c)}{\le} \frac{1}{a_{\mathrm{m},\ell}^{\boldsymbol{\nabla} u,k}} \left(\int_{|\boldsymbol{\nabla} u|}^{|\boldsymbol{\nabla} u_\ell^k|} \phi''(\cdot, r)\,\mathrm{d}r \right)^2 \overset{(A.2)}{=} \frac{1}{a_{\mathrm{m},\ell}^{\boldsymbol{\nabla} u,k}} \left(|a_\ell^k \boldsymbol{\nabla} u_\ell^k| - |a_u \boldsymbol{\nabla} u| \right)^2.
\end{aligned}
\tag{7.7}
$$

Hence, observing again that $|\boldsymbol{\nabla} u_\ell^k||\boldsymbol{\nabla} u| - \boldsymbol{\nabla} u_\ell^k \cdot \boldsymbol{\nabla} u \ge 0$ thanks to the Cauchy–Schwarz inequality, we obtain the right-hand side of (4.4c) by writing

$$
\begin{aligned}
(\mathcal{E}^k_{\mathrm{N},\ell})^2 &\overset{(7.3),(7.7),(4.3c)}{\leq} \int_\Omega \frac{2}{a^{\nabla u,k}_{\mathrm{m},\ell}}\Big(\big(|a^k_\ell \nabla u^k_\ell| - |a_u \nabla u|\big)^2 + 2(|a^k_\ell \nabla u^k_\ell||a_u \nabla u| \\
&\qquad - (a^k_\ell \nabla u^k_\ell)\cdot(a_u \nabla u)\big)\Big) \overset{(A.4a)}{=} \int_\Omega \frac{2}{a^{\nabla u,k}_{\mathrm{m},\ell}} |a^k_\ell \nabla u^k_\ell - a_u \nabla u|^2.
\end{aligned} \tag{7.8}
$$

□

8 Proof of Theorem 4.4

For all vertices $\boldsymbol{a} \in \mathcal{V}_\ell$, we introduce the space $H^1_*(\omega^{\boldsymbol{a}}_\ell)$ such that

$$
H^1_*(\omega^{\boldsymbol{a}}_\ell) := \begin{cases} \{\varphi \in H^1(\omega^{\boldsymbol{a}}_\ell) : (\varphi, 1)_{\omega^{\boldsymbol{a}}_\ell} = 0\} & \text{if } \boldsymbol{a} \in \mathcal{V}^{\mathrm{int}}_\ell, \\ \{\varphi \in H^1(\omega^{\boldsymbol{a}}_\ell) : \varphi_{|\partial\omega^{\boldsymbol{a}}_\ell \cap \{\psi^{\boldsymbol{a}}_\ell > 0\}} = 0\} & \text{if } \boldsymbol{a} \notin \mathcal{V}^{\mathrm{int}}_\ell, \end{cases} \tag{8.1}
$$

where $\mathcal{V}^{\mathrm{int}}_\ell$ is the set of the vertices of $\mathcal{T}_\ell$ lying inside Ω. We will need:

Lemma 8.1 (Patchwise flux equilibration stability)**.** *Let $\boldsymbol{a} \in \mathcal{V}_\ell$ and let $\boldsymbol{\tau}^{\boldsymbol{a}}_\ell \in \boldsymbol{RTN}_p(\mathcal{T}^{\boldsymbol{a}}_\ell)$ and $g^{\boldsymbol{a}}_\ell \in \mathcal{P}_p(\mathcal{T}^{\boldsymbol{a}}_\ell)$ be such that $(g^{\boldsymbol{a}}_\ell, 1)_{\omega^{\boldsymbol{a}}_\ell} = 0$ if $\boldsymbol{a} \in \mathcal{V}^{\mathrm{int}}_\ell$. Then,*

$$
\min_{\substack{\boldsymbol{v}^{\boldsymbol{a}}_\ell \in \boldsymbol{V}^{\boldsymbol{a}}_\ell \\ \nabla\cdot \boldsymbol{v}^{\boldsymbol{a}}_\ell = g^{\boldsymbol{a}}_\ell}} \|\boldsymbol{v}^{\boldsymbol{a}}_\ell + \boldsymbol{\tau}^{\boldsymbol{a}}_\ell\|_{\omega^{\boldsymbol{a}}_\ell} \lesssim \sup_{\substack{\varphi \in H^1_*(\omega^{\boldsymbol{a}}_\ell) \\ \|\nabla\varphi\|_{\omega^{\boldsymbol{a}}_\ell} = 1}} \left[(g^{\boldsymbol{a}}_\ell, \varphi)_{\omega^{\boldsymbol{a}}_\ell} - (\boldsymbol{\tau}^{\boldsymbol{a}}_\ell, \nabla\varphi)_{\omega^{\boldsymbol{a}}_\ell}\right], \tag{8.2}
$$

where the hidden constant only depends on the space dimension d, the mesh shape-regularity $\kappa_{\mathcal{T}}$, and possibly, when $d \geq 4$, the polynomial degree p.

Proof. See [21, Corollary 3.3] or [19, Lemma 3.2]. □

We will use next the fact that, for all $\boldsymbol{v} \in \boldsymbol{L}^2(\Omega)$ and $\boldsymbol{W} \in [L^2(\Omega)]^{d\times d}$,

$$
\sum_{a \in \mathcal{V}_\ell} \|\boldsymbol{v}\|^2_{\omega^{\boldsymbol{a}}_\ell} = \sum_{K \in \mathcal{T}_\ell} \sum_{a \in \mathcal{V}_K} \|\boldsymbol{v}\|^2_K = (d+1) \sum_{K \in \mathcal{T}_\ell} \|\boldsymbol{v}\|^2_K = (d+1)\|\boldsymbol{v}\|^2, \tag{8.3}
$$

since every simplex $K \in \mathcal{T}_\ell$ has $(d+1)$ vertices, collected in the set $\mathcal{V}_K$. Also,

$$
\begin{aligned}
\|\boldsymbol{v} + \boldsymbol{W}\boldsymbol{\sigma}^k_\ell\|^2 &= \sum_{K \in \mathcal{T}_\ell} \|\boldsymbol{v} + \boldsymbol{W}\boldsymbol{\sigma}^k_\ell\|^2_K \overset{(3.5),(3.6a)}{=} \sum_{K \in \mathcal{T}_\ell} \Big\| \sum_{a \in \mathcal{V}_K} (\psi^{\boldsymbol{a}}_\ell \boldsymbol{v} + \boldsymbol{W}\boldsymbol{\sigma}^{\boldsymbol{a},k}_\ell) \Big\|^2_K \\
&\leq (d+1) \sum_{K \in \mathcal{T}_\ell} \sum_{a \in \mathcal{V}_K} \|\psi^{\boldsymbol{a}}_\ell \boldsymbol{v} + \boldsymbol{W}\boldsymbol{\sigma}^{\boldsymbol{a},k}_\ell\|^2_K = (d+1) \sum_{a \in \mathcal{V}_\ell} \|\psi^{\boldsymbol{a}}_\ell \boldsymbol{v} + \boldsymbol{W}\boldsymbol{\sigma}^{\boldsymbol{a},k}_\ell\|^2_{\omega^{\boldsymbol{a}}_\ell}.
\end{aligned} \tag{8.4}
$$

In the following, for any $x, y \in [0, \infty)$, we use the notation $x \lesssim y$ when $x \leq Cy$ with $C \geq 0$ only depending on the space dimension d, the mesh shape-regularity $\kappa_{\mathcal{T}}$, and possibly, when $d \geq 4$, the polynomial degree p.

Proof of Theorem 4.4. As in [2, 41, 45] but including data oscillations, we have

$$
\begin{aligned}
(\mathcal{E}^k_{\mathrm{N},\ell})^2 &\overset{(4.1)}{=} (\eta^k_{\mathrm{N},\ell})^2 - 2\int_\Omega (\phi^*(|\boldsymbol{\sigma}^k_\ell|) + \phi(|\nabla u|) - fu) \\
&\overset{(3.2a)}{\leq} (\eta^k_{\mathrm{N},\ell})^2 - 2\int_\Omega (|\boldsymbol{\sigma}^k_\ell||\nabla u| - fu) \leq (\eta^k_{\mathrm{N},\ell})^2 + 2((f,u) + (\boldsymbol{\sigma}^k_\ell, \nabla u)) \\
&\overset{(3.9)}{=} (\eta^k_{\mathrm{N},\ell})^2 + 2(f - \nabla\cdot\boldsymbol{\sigma}^k_\ell, u - u^k_\ell) \\
&\overset{(3.8)}{\leq} (\eta^k_{\mathrm{N},\ell})^2 + 2\left(\sum_{K \in \mathcal{T}_\ell} \left[\frac{h_K}{\pi}\|f - \Pi_{\ell,p} f\|_K\right]^2\right)^{\frac{1}{2}} \|\nabla(u - u^k_\ell)\| \\
&\overset{(9.3),(4.5a)}{\leq} (\eta^k_{\mathrm{N},\ell})^2 + 2\eta^k_{\mathrm{osc},\ell}\mathcal{E}^k_{\mathrm{N},\ell}.
\end{aligned} \tag{8.5}
$$

By the quadratic formula, this gives

$$\mathcal{E}_{\mathrm{N},\ell}^{k} \leq \frac{1}{2}\left(2\eta_{\mathrm{osc},\ell}^{k} + (4(\eta_{\mathrm{osc},\ell}^{k})^2 + 4(\eta_{\mathrm{N},\ell}^{k})^2)^{\frac{1}{2}}\right) \leq \eta_{\mathrm{N},\ell}^{k} + 2\eta_{\mathrm{osc},\ell}^{k}, \tag{8.6}$$

hence (4.7a).

It remains to prove (4.7b). Let us temporarily denote $\varsigma := 1/(\operatorname{ess\,inf}_{\omega_\ell^{\boldsymbol{a}}} a_{\mathrm{m},\ell}^{\boldsymbol{\sigma},k})^{\frac{1}{2}}$ the weight appearing in (4.5c)–(4.5d). We apply the triangle inequality, the definitions (4.5c)–(4.5d), the fact that $0 \leq \psi_\ell^{\boldsymbol{a}} \leq 1$, the definition (3.6b) with the choice (3.7a), and Lemma 8.1 with $\boldsymbol{\tau}_\ell^{\boldsymbol{a}} = \psi_\ell^{\boldsymbol{a}} \boldsymbol{\Pi}_{\ell,p-1}^{\boldsymbol{RTN}} \boldsymbol{\xi}_\ell^k \in \boldsymbol{RTN}_p(\mathcal{T}_\ell^{\boldsymbol{a}})$ and $g_\ell^{\boldsymbol{a}} = \Pi_{\ell,p}\gamma_\ell^{\boldsymbol{a},k} \in \mathcal{P}_p(\mathcal{T}_\ell^{\boldsymbol{a}})$ with $(g_\ell^{\boldsymbol{a}}, 1)_{\omega_\ell^{\boldsymbol{a}}} = 0$ if $\boldsymbol{a} \in \mathcal{V}_\ell^{\mathrm{int}}$. Also using the fact that $\psi_\ell^{\boldsymbol{a}}\varphi \in H_0^1(\omega_\ell^{\boldsymbol{a}})$ and $\boldsymbol{\nabla}(\psi_\ell^{\boldsymbol{a}}\varphi) = \psi_\ell^{\boldsymbol{a}}\boldsymbol{\nabla}\varphi + \varphi\boldsymbol{\nabla}\psi_\ell^{\boldsymbol{a}}$ for all $\varphi \in H_*^1(\omega_\ell^{\boldsymbol{a}})$, we get

$$\begin{aligned}
\varsigma\|\psi_\ell^{\boldsymbol{a}} a_\ell^k \boldsymbol{\nabla} u_\ell^k + \boldsymbol{\sigma}_\ell^{\boldsymbol{a},k}\|_{\omega_\ell^{\boldsymbol{a}}} &\overset{(4.5)}{\leq} \varsigma\|\psi_\ell^{\boldsymbol{a}} \boldsymbol{\Pi}_{\ell,p-1}^{\boldsymbol{RTN}} \boldsymbol{\xi}_\ell^k + \boldsymbol{\sigma}_\ell^{\boldsymbol{a},k}\|_{\omega_\ell^{\boldsymbol{a}}} + \eta_{\mathrm{osc,q},\ell}^{\boldsymbol{a},k} + \eta_{\mathrm{iter},\ell}^{\boldsymbol{a},k} \\
&\overset{(3.6b),(8.2)}{\lesssim} \varsigma \sup_{\substack{\varphi \in H_*^1(\omega_\ell^{\boldsymbol{a}}) \\ \|\boldsymbol{\nabla}\varphi\|_{\omega_\ell^{\boldsymbol{a}}}=1}} \left[(\Pi_{\ell,p}\gamma_\ell^{\boldsymbol{a},k}, \varphi)_{\omega_\ell^{\boldsymbol{a}}} - (\psi_\ell^{\boldsymbol{a}} \boldsymbol{\Pi}_{\ell,p-1}^{\boldsymbol{RTN}} \boldsymbol{\xi}_\ell^k, \boldsymbol{\nabla}\varphi)_{\omega_\ell^{\boldsymbol{a}}}\right] + \eta_{\mathrm{osc,q},\ell}^{\boldsymbol{a},k} + \eta_{\mathrm{iter},\ell}^{\boldsymbol{a},k} \\
&\overset{(3.6b),(4.5c)}{\lesssim} \varsigma \sup_{\substack{\varphi \in H_*^1(\omega_\ell^{\boldsymbol{a}}) \\ \|\boldsymbol{\nabla}\varphi\|_{\omega_\ell^{\boldsymbol{a}}}=1}} \left[(f, \psi_\ell^{\boldsymbol{a}}\varphi)_{\omega_\ell^{\boldsymbol{a}}} - (\boldsymbol{\xi}_\ell^k, \boldsymbol{\nabla}(\psi_\ell^{\boldsymbol{a}}\varphi))_{\omega_\ell^{\boldsymbol{a}}}\right] + \eta_{\mathrm{osc,q},\ell}^{\boldsymbol{a},k} + \eta_{\mathrm{iter},\ell}^{\boldsymbol{a},k} \\
&\overset{(4.5d)}{\lesssim} \varsigma \sup_{\substack{\varphi \in H_*^1(\omega_\ell^{\boldsymbol{a}}) \\ \|\boldsymbol{\nabla}\varphi\|_{\omega_\ell^{\boldsymbol{a}}}=1}} \left[(f, \psi_\ell^{\boldsymbol{a}}\varphi)_{\omega_\ell^{\boldsymbol{a}}} - (a_\ell^k \boldsymbol{\nabla} u_\ell^k, \boldsymbol{\nabla}(\psi_\ell^{\boldsymbol{a}}\varphi))_{\omega_\ell^{\boldsymbol{a}}}\right] + \eta_{\mathrm{osc,q},\ell}^{\boldsymbol{a},k} + \eta_{\mathrm{iter},\ell}^{\boldsymbol{a},k} \\
&\overset{(2.2a)}{=} \varsigma \sup_{\substack{\varphi \in H_*^1(\omega_\ell^{\boldsymbol{a}}) \\ \|\boldsymbol{\nabla}\varphi\|_{\omega_\ell^{\boldsymbol{a}}}=1}} (a_u \boldsymbol{\nabla} u - a_\ell^k \boldsymbol{\nabla} u_\ell^k, \boldsymbol{\nabla}(\psi_\ell^{\boldsymbol{a}}\varphi))_{\omega_\ell^{\boldsymbol{a}}} + \eta_{\mathrm{osc,q},\ell}^{\boldsymbol{a},k} + \eta_{\mathrm{iter},\ell}^{\boldsymbol{a},k} \\
&\lesssim \varsigma\|a_\ell^k \boldsymbol{\nabla} u_\ell^k - a_u \boldsymbol{\nabla} u\|_{\omega_\ell^{\boldsymbol{a}}} + \eta_{\mathrm{osc,q},\ell}^{\boldsymbol{a},k} + \eta_{\mathrm{iter},\ell}^{\boldsymbol{a},k},
\end{aligned} \tag{8.7}$$

where we have used $\|\boldsymbol{\nabla}(\psi_\ell^{\boldsymbol{a}}\varphi)\|_{\omega_\ell^{\boldsymbol{a}}} \lesssim \|\boldsymbol{\nabla}\varphi\|_{\omega_\ell^{\boldsymbol{a}}}$ as in [8, 19]. In conclusion, we obtain

$$\begin{aligned}
\eta_{\mathrm{N},\ell}^{k} &\overset{(4.4b),(8.4)}{\lesssim} \left(\sum_{\boldsymbol{a} \in \mathcal{V}_\ell} \frac{1}{\operatorname{ess\,inf}_{\omega_\ell^{\boldsymbol{a}}} a_{\mathrm{m},\ell}^{\boldsymbol{\sigma},k}} \|\psi_\ell^{\boldsymbol{a}} a_\ell^k \boldsymbol{\nabla} u_\ell^k + \boldsymbol{\sigma}_\ell^{\boldsymbol{a},k}\|_{\omega_\ell^{\boldsymbol{a}}}^2\right)^{\frac{1}{2}} \\
&\overset{(8.7),(4.5)}{\lesssim} \left(\sum_{\boldsymbol{a} \in \mathcal{V}_\ell} \frac{1}{\operatorname{ess\,inf}_{\omega_\ell^{\boldsymbol{a}}} a_{\mathrm{m},\ell}^{\boldsymbol{\sigma},k}} \|a_\ell^k \boldsymbol{\nabla} u_\ell^k - a_u \boldsymbol{\nabla} u\|_{\omega_\ell^{\boldsymbol{a}}}^2\right)^{\frac{1}{2}} + \eta_{\mathrm{osc,q},\ell}^{k} + \eta_{\mathrm{iter},\ell}^{k} \\
&\overset{(4.8)}{\leq} C_\ell^k \left(\sum_{\boldsymbol{a} \in \mathcal{V}_\ell} \frac{1}{\operatorname{ess\,sup}_{\omega_\ell^{\boldsymbol{a}}} a_{\mathrm{c},\ell}^{\boldsymbol{\nabla}u,k}} \|a_\ell^k \boldsymbol{\nabla} u_\ell^k - a_u \boldsymbol{\nabla} u\|_{\omega_\ell^{\boldsymbol{a}}}^2\right)^{\frac{1}{2}} + \eta_{\mathrm{osc,q},\ell}^{k} + \eta_{\mathrm{iter},\ell}^{k} \\
&\overset{(8.3),(4.4c)}{\lesssim} C_\ell^k \mathcal{E}_{\mathrm{N},\ell}^k + \eta_{\mathrm{osc,q},\ell}^{k} + \eta_{\mathrm{iter},\ell}^{k},
\end{aligned} \tag{8.8}$$

where we have used the triangle inequality on $\ell_2(\mathbb{R}^{|\mathcal{V}_\ell|})$. □

9 Proof of Lemmas 5.1 and 5.3

Proof of Lemma 5.1. We write with the triangle inequality

$$\begin{aligned}
\eta_{\mathrm{N},\ell}^{k} &\overset{(7.2)}{\leq} \|(a_{\mathrm{m},\ell}^{\boldsymbol{\sigma},k})^{-\frac{1}{2}}(a_\ell^k \boldsymbol{\nabla} u_\ell^k + \boldsymbol{\sigma}_\ell^k)\| \overset{(4.3),(2.8)}{\leq} a_{\mathrm{m}}^{-\frac{1}{2}} A_{\mathrm{c}}^{\frac{1}{2}} \|(\boldsymbol{A}_\ell^{k-1})^{-\frac{1}{2}}(a_\ell^k \boldsymbol{\nabla} u_\ell^k + \boldsymbol{\sigma}_\ell^k)\| \\
&\leq a_{\mathrm{m}}^{-\frac{1}{2}} A_{\mathrm{c}}^{\frac{1}{2}} \Big(\|(\boldsymbol{A}_\ell^{k-1})^{-\frac{1}{2}}(\boldsymbol{A}_\ell^{k-1}\boldsymbol{\nabla}(u_\ell^k - u_\ell^{k-1}) + a_\ell^{k-1}\boldsymbol{\nabla} u_\ell^{k-1} + \boldsymbol{\sigma}_\ell^k)\| \\
&\qquad + \|(\boldsymbol{A}_\ell^{k-1})^{-\frac{1}{2}}(a_\ell^k \boldsymbol{\nabla} u_\ell^k - a_\ell^{k-1}\boldsymbol{\nabla} u_\ell^{k-1} - \boldsymbol{A}_\ell^{k-1}\boldsymbol{\nabla}(u_\ell^k - u_\ell^{k-1}))\|\Big) \\
&\overset{(5.2b),(5.3)}{=} a_{\mathrm{m}}^{-\frac{1}{2}} A_{\mathrm{c}}^{\frac{1}{2}} (\eta_{\mathrm{L},\ell}^k + \widehat{\eta}_{\mathrm{iter},\ell}^k),
\end{aligned} \tag{9.1}$$

where we have also employed the definitions (2.9) and (3.6b). Thus, by virtue of the definition (5.4), λ_ℓ^k is uniformly bounded as per (5.6). □

Proof of Lemma 5.3. The first two inequalities in (5.8) are immediate from (5.5) and (5.6). As for the last one, for all $k \geq 1$,

$$
\begin{aligned}
A_{\mathrm{m}}\|\boldsymbol{\nabla}(u_{\langle\ell\rangle}^{k}-u_{\ell}^{k-1})\|^{2} &\overset{(2.8)}{\leq} (\boldsymbol{A}_{\ell}^{k-1}\boldsymbol{\nabla}(u_{\langle\ell\rangle}^{k}-u_{\ell}^{k-1}),\boldsymbol{\nabla}(u_{\langle\ell\rangle}^{k}-u_{\ell}^{k-1}))\\
&\overset{(2.9)}{=} (\boldsymbol{A}_{\ell}^{k-1}\boldsymbol{\nabla}u_{\langle\ell\rangle}^{k}-\boldsymbol{b}_{\ell}^{k-1},\boldsymbol{\nabla}(u_{\langle\ell\rangle}^{k}-u_{\ell}^{k-1}))-(a_{\ell}^{k-1}\boldsymbol{\nabla}u_{\ell}^{k-1},\boldsymbol{\nabla}(u_{\langle\ell\rangle}^{k}-u_{\ell}^{k-1}))\\
&\overset{(5.1a)}{=} (f,u_{\langle\ell\rangle}^{k}-u_{\ell}^{k-1})-(a_{\ell}^{k-1}\boldsymbol{\nabla}u_{\ell}^{k-1},\boldsymbol{\nabla}(u_{\langle\ell\rangle}^{k}-u_{\ell}^{k-1}))\\
&\overset{(2.2a)}{=} (a_{u}\boldsymbol{\nabla}u-a_{\ell}^{k-1}\boldsymbol{\nabla}u_{\ell}^{k-1},\boldsymbol{\nabla}(u_{\langle\ell\rangle}^{k}-u_{\ell}^{k-1}))\\
&\overset{(2.1a)}{\leq} a_{\mathrm{c}}\|\boldsymbol{\nabla}(u-u_{\ell}^{k-1})\|\|\boldsymbol{\nabla}(u_{\langle\ell\rangle}^{k}-u_{\ell}^{k-1})\|.
\end{aligned}
\tag{9.2}
$$

Hence, dividing (9.2) by $\|\boldsymbol{\nabla}(u_{\langle\ell\rangle}^{k}-u_{\ell}^{k-1})\|$, we infer

$$
A_{\mathrm{m}}a_{\mathrm{c}}^{-1}\|\boldsymbol{\nabla}(u_{\langle\ell\rangle}^{k}-u_{\ell}^{k-1})\| \leq \|\boldsymbol{\nabla}(u-u_{\ell}^{k-1})\|,
$$

and consequently, by the triangle inequality,

$$
A_{\mathrm{m}}a_{\mathrm{c}}^{-1}\|\boldsymbol{\nabla}(u_{\langle\ell\rangle}^{k}-u_{\ell}^{k})\| \leq \|\boldsymbol{\nabla}(u-u_{\ell}^{k})\|+\|\boldsymbol{\nabla}(u_{\ell}^{k}-u_{\ell}^{k-1})\|+A_{\mathrm{m}}a_{\mathrm{c}}^{-1}\|\boldsymbol{\nabla}(u_{\ell}^{k}-u_{\ell}^{k-1})\|.
$$

Thus, $\mathcal{E}_{\mathrm{L},\ell}^{k} \lesssim \mathcal{E}_{\mathrm{N},\ell}^{k}+\|\boldsymbol{\nabla}(u_{\ell}^{k}-u_{\ell}^{k-1})\|$ thanks to definition (5.2a) (employing the relation (10.1a) below) and

$$
a_{\mathrm{m}}\|\boldsymbol{\nabla}(u_{\ell}^{k}-u)\|^{2} \leq (\mathcal{E}_{\mathrm{N},\ell}^{k})^{2} \leq a_{\mathrm{c}}\|\boldsymbol{\nabla}(u_{\ell}^{k}-u)\|^{2}, \tag{9.3}
$$

which is a consequence of inequality (4.4a) together with the bounds in (4.3).

The convergence statement is then easy. Assuming $\mathcal{E}_{\ell}^{k} \to 0$ implies $\mathcal{E}_{\mathrm{N},\ell}^{k} \to 0$ and then the $H_0^1(\Omega)$ convergence follows from (9.3). Reciprocally, when $u_{\ell}^{k} \to u$ in $H_0^1(\Omega)$, the last term in (5.8) goes to 0, as well as $\mathcal{E}_{\mathrm{N},\ell}^{k}$ thanks to (9.3), so that $\mathcal{E}_{\ell}^{k} \to 0$. □

10 Proof of Theorem 5.5

Recalling the definition (2.7) of $\mathcal{J}_{\ell}^{k-1}$, we can rewrite $\mathcal{E}_{\mathrm{L},\ell}^{k}$ given by (5.2a) as

$$
\begin{aligned}
(\mathcal{E}_{\mathrm{L},\ell}^{k})^{2} &\overset{(2.7)}{=} \left\|(\boldsymbol{A}_{\ell}^{k-1})^{\frac{1}{2}}\boldsymbol{\nabla}u_{\ell}^{k}\right\|^{2}-\left\|(\boldsymbol{A}_{\ell}^{k-1})^{\frac{1}{2}}\boldsymbol{\nabla}u_{\langle\ell\rangle}^{k}\right\|^{2}\\
&\qquad -2(\boldsymbol{b}_{\ell}^{k-1},\boldsymbol{\nabla}(u_{\ell}^{k}-u_{\langle\ell\rangle}^{k}))-2(f,u_{\ell}^{k}-u_{\langle\ell\rangle}^{k})\\
&\overset{(5.1a)}{=} \left\|(\boldsymbol{A}_{\ell}^{k-1})^{\frac{1}{2}}\boldsymbol{\nabla}u_{\ell}^{k}\right\|^{2}-\left\|(\boldsymbol{A}_{\ell}^{k-1})^{\frac{1}{2}}\boldsymbol{\nabla}u_{\langle\ell\rangle}^{k}\right\|^{2}-2(\boldsymbol{A}_{\ell}^{k-1}\boldsymbol{\nabla}u_{\langle\ell\rangle}^{k},\boldsymbol{\nabla}(u_{\ell}^{k}-u_{\langle\ell\rangle}^{k}))\\
&= \|(\boldsymbol{A}_{\ell}^{k-1})^{\frac{1}{2}}\boldsymbol{\nabla}(u_{\ell}^{k}-u_{\langle\ell\rangle}^{k})\|^{2} \overset{(8.3)}{=} \frac{1}{d+1}\sum_{\boldsymbol{a}\in\mathcal{V}_{\ell}}(\mathcal{E}_{\mathrm{L},\ell}^{\boldsymbol{a},k})^{2},
\end{aligned}
\tag{10.1a}
$$

where, for all $\boldsymbol{a} \in \mathcal{V}_{\ell}$,

$$
\mathcal{E}_{\mathrm{L},\ell}^{\boldsymbol{a},k} \coloneqq \|(\boldsymbol{A}_{\ell}^{k-1})^{\frac{1}{2}}\boldsymbol{\nabla}(u_{\ell}^{k}-u_{\langle\ell\rangle}^{k})\|_{\omega_{\ell}^{\boldsymbol{a}}}. \tag{10.1b}
$$

Similarly, using the definition (3.4) of $\mathcal{J}_{\ell}^{*,k-1}$, we can rewrite and upper-bound $\eta_{\mathrm{L},\ell}^{k}$ of (5.2b),

$$
\begin{aligned}
(\eta_{\mathrm{L},\ell}^{k})^{2} &\overset{(3.4)}{=} \left\|(\boldsymbol{A}_{\ell}^{k-1})^{\frac{1}{2}}\boldsymbol{\nabla}u_{\ell}^{k}\right\|^{2}+\left\|(\boldsymbol{A}_{\ell}^{k-1})^{-\frac{1}{2}}(\boldsymbol{\sigma}_{\ell}^{k}-\boldsymbol{b}_{\ell}^{k-1})\right\|^{2}-2(\boldsymbol{b}_{\ell}^{k-1},\boldsymbol{\nabla}u_{\ell}^{k})-2(f,u_{\ell}^{k})\\
&= \|(\boldsymbol{A}_{\ell}^{k-1})^{-\frac{1}{2}}(\boldsymbol{A}_{\ell}^{k-1}\boldsymbol{\nabla}u_{\ell}^{k}-\boldsymbol{b}_{\ell}^{k-1}+\boldsymbol{\sigma}_{\ell}^{k})\|^{2}-2(\boldsymbol{\sigma}_{\ell}^{k},\boldsymbol{\nabla}u_{\ell}^{k})-2(f,u_{\ell}^{k})\\
&\overset{(3.9)}{=} \|(\boldsymbol{A}_{\ell}^{k-1})^{-\frac{1}{2}}(\boldsymbol{A}_{\ell}^{k-1}\boldsymbol{\nabla}u_{\ell}^{k}-\boldsymbol{b}_{\ell}^{k-1}+\boldsymbol{\sigma}_{\ell}^{k})\|^{2} \overset{(8.4)}{\leq} (d+1)\sum_{\boldsymbol{a}\in\mathcal{V}_{\ell}}(\eta_{\mathrm{L},\ell}^{\boldsymbol{a},k})^{2},
\end{aligned}
\tag{10.2a}
$$

where, for all $\boldsymbol{a} \in \mathcal{V}_{\ell}$,

$$
\eta_{\mathrm{L},\ell}^{\boldsymbol{a},k} \coloneqq \|(\boldsymbol{A}_{\ell}^{k-1})^{-\frac{1}{2}}(\psi_{\ell}^{\boldsymbol{a}}(\boldsymbol{A}_{\ell}^{k-1}\boldsymbol{\nabla}u_{\ell}^{k}-\boldsymbol{b}_{\ell}^{k-1})+\boldsymbol{\sigma}_{\ell}^{\boldsymbol{a},k})\|_{\omega_{\ell}^{\boldsymbol{a}}}. \tag{10.2b}
$$

Proof of Theorem 5.5. Let $k \geq 1$. Since (5.1) is a linear problem, proceeding as in [19, 20], we obtain the a posteriori error estimate

$$\begin{aligned}
(\mathcal{E}^k_{\mathrm{L},\ell})^2 &\overset{(10.1a)}{=} (\boldsymbol{A}^{k-1}_\ell \boldsymbol{\nabla}(u^k_{\langle\ell\rangle} - u^k_\ell), \boldsymbol{\nabla}(u^k_{\langle\ell\rangle} - u^k_\ell)) \\
&\overset{(5.1a)}{=} (f, u^k_{\langle\ell\rangle} - u^k_\ell) - (\boldsymbol{A}^{k-1}_\ell \boldsymbol{\nabla} u^k_\ell - \boldsymbol{b}^{k-1}_\ell, \boldsymbol{\nabla}(u^k_{\langle\ell\rangle} - u^k_\ell)) \\
&\overset{(3.8)}{=} ((I - \Pi_{\ell,p})f, u^k_{\langle\ell\rangle} - u^k_\ell) - (\boldsymbol{A}^{k-1}_\ell \boldsymbol{\nabla} u^k_\ell - \boldsymbol{b}^{k-1}_\ell + \boldsymbol{\sigma}^k_\ell, \boldsymbol{\nabla}(u^k_{\langle\ell\rangle} - u^k_\ell)) \\
&\overset{(5.9a)}{\leq} (\widehat{\eta}^k_{\mathrm{osc},\ell} + \|(\boldsymbol{A}^{k-1}_\ell)^{-\frac{1}{2}}(\boldsymbol{A}^{k-1}_\ell \boldsymbol{\nabla} u^k_\ell - \boldsymbol{b}^{k-1}_\ell + \boldsymbol{\sigma}^k_\ell)\|)\|(\boldsymbol{A}^{k-1}_\ell)^{\frac{1}{2}}\boldsymbol{\nabla}(u^k_\ell - u^k_{\langle\ell\rangle})\| \\
&\overset{(10.1a),(10.2a)}{=} (\widehat{\eta}^k_{\mathrm{osc},\ell} + \eta^k_{\mathrm{L},\ell})\mathcal{E}^k_{\mathrm{L},\ell}.
\end{aligned} \tag{10.3}$$

Now, observing that (8.6) still holds with the version (3.7b) of the equilibrated flux, we obtain (5.10a) by writing

$$\begin{aligned}
\mathcal{E}^k_\ell &\overset{(5.5)}{=} \frac{1}{2}(\mathcal{E}^k_{\mathrm{N},\ell} + \lambda^k_\ell \mathcal{E}^k_{\mathrm{L},\ell}) \\
&\overset{(8.6),(10.3)}{\leq} \frac{1}{2}(\eta^k_{\mathrm{N},\ell} + 2\eta^k_{\mathrm{osc},\ell} + \lambda^k_\ell(\eta^k_{\mathrm{L},\ell} + \widehat{\eta}^k_{\mathrm{osc},\ell})) \\
&\overset{(5.5)}{=} \eta^k_\ell + \eta^k_{\mathrm{osc},\ell} + \frac{\lambda^k_\ell}{2}\widehat{\eta}^k_{\mathrm{osc},\ell}.
\end{aligned} \tag{10.4}$$

It remains to prove (5.10b). For all vertices $\boldsymbol{a} \in \mathcal{V}_\ell$, denote by $\boldsymbol{\sigma}^{\boldsymbol{a},k}_{\mathrm{I},\ell}$ the minimizer of (3.6b) with the choice (3.7a). Recall also the notations (10.2b) and (3.6b) together with (5.9c) and (5.9d). Then, using the same reasoning as in (8.7), we infer

$$\begin{aligned}
\eta^{\boldsymbol{a},k}_{\mathrm{L},\ell} &\overset{(5.9d)}{\leq} \|(\boldsymbol{A}^{k-1}_\ell)^{-\frac{1}{2}}(\psi^{\boldsymbol{a}}_\ell \boldsymbol{\Pi}^{\boldsymbol{RTN}}_{\ell,p-1}\boldsymbol{\xi}^k_\ell + \boldsymbol{\sigma}^{\boldsymbol{a},k}_\ell)\|_{\omega^{\boldsymbol{a}}_\ell} + \widehat{\eta}^{\boldsymbol{a},k}_{\mathrm{q},\ell} \\
&\overset{(2.8)}{\leq} \frac{1}{(\inf_{\omega^{\boldsymbol{a}}_\ell} A^{k-1}_{\mathrm{m},\ell})^{\frac{1}{2}}}\|\psi^{\boldsymbol{a}}_\ell \boldsymbol{\Pi}^{\boldsymbol{RTN}}_{\ell,p-1}\boldsymbol{\xi}^k_\ell + \boldsymbol{\sigma}^{\boldsymbol{a},k}_{\mathrm{I},\ell}\|_{\omega^{\boldsymbol{a}}_\ell} + \widehat{\eta}^{\boldsymbol{a},k}_{\mathrm{q},\ell} \\
&\overset{(8.7),(5.11)}{\lesssim} \frac{1}{(\inf_{\omega^{\boldsymbol{a}}_\ell} A^{k-1}_{\mathrm{m},\ell})^{\frac{1}{2}}} \sup_{\substack{\varphi \in H^1_*(\omega^{\boldsymbol{a}}_\ell) \\ \|\boldsymbol{\nabla}\varphi\|_{\omega^{\boldsymbol{a}}_\ell} = 1}} \left[(f, \psi^{\boldsymbol{a}}_\ell \varphi)_{\omega^{\boldsymbol{a}}_\ell} - (\boldsymbol{\xi}^k_\ell, \boldsymbol{\nabla}(\psi^{\boldsymbol{a}}_\ell \varphi))_{\omega^{\boldsymbol{a}}_\ell}\right] \\
&\qquad + (1 + \widehat{C}^k_\ell)\widehat{\eta}^{\boldsymbol{a},k}_{\mathrm{q},\ell} + \widehat{\eta}^{\boldsymbol{a},k}_{\mathrm{osc,q},\ell} \\
&\overset{(5.1a),(10.1b)}{\lesssim} \widehat{C}^k_\ell \mathcal{E}^{\boldsymbol{a},k}_{\mathrm{L},\ell} + \widehat{C}^k_\ell \widehat{\eta}^{\boldsymbol{a},k}_{\mathrm{q},\ell} + \widehat{\eta}^{\boldsymbol{a},k}_{\mathrm{osc,q},\ell}.
\end{aligned} \tag{10.5}$$

Therefore, we obtain (5.10b) by writing

$$\begin{aligned}
2\eta^k_\ell &\overset{(5.5)}{=} \eta^k_{\mathrm{N},\ell} + \lambda^k_\ell \eta^k_{\mathrm{L},\ell} \overset{(5.4)}{=} \lambda^k_\ell(2\eta^k_{\mathrm{L},\ell} + \widehat{\eta}^k_{\mathrm{iter},\ell}) \\
&\overset{(10.2)}{\lesssim} \lambda^k_\ell \Bigg(\sum_{\boldsymbol{a}\in\mathcal{V}_\ell} (\eta^{\boldsymbol{a},k}_{\mathrm{L},\ell})^2\Bigg)^{\frac{1}{2}} + \lambda^k_\ell \widehat{\eta}^k_{\mathrm{iter},\ell} \\
&\overset{(10.5)}{\lesssim} \lambda^k_\ell \left[\widehat{C}^k_\ell \Bigg(\sum_{\boldsymbol{a}\in\mathcal{V}_\ell} (\mathcal{E}^{\boldsymbol{a},k}_{\mathrm{L},\ell})^2\Bigg)^{\frac{1}{2}} + \widehat{C}^k_\ell \Bigg(\sum_{\boldsymbol{a}\in\mathcal{V}_\ell} (\widehat{\eta}^{\boldsymbol{a},k}_{\mathrm{q},\ell})^2\Bigg)^{\frac{1}{2}} + \Bigg(\sum_{\boldsymbol{a}\in\mathcal{V}_\ell} (\widehat{\eta}^{\boldsymbol{a},k}_{\mathrm{osc,q},\ell})^2\Bigg)^{\frac{1}{2}}\right] \\
&\qquad + \lambda^k_\ell \widehat{\eta}^k_{\mathrm{iter},\ell} \\
&\overset{(10.1),(5.9)}{\lesssim} \lambda^k_\ell \left[\frac{1}{2}\widehat{C}^k_\ell \mathcal{E}^k_{\mathrm{L},\ell} + \widehat{C}^k_\ell \widehat{\eta}^k_{\mathrm{q},\ell} + \widehat{\eta}^k_{\mathrm{osc,q},\ell} + \widehat{\eta}^k_{\mathrm{iter},\ell}\right] \\
&\overset{(5.5)}{\leq} \widehat{C}^k_\ell \mathcal{E}^k_\ell + \lambda^k_\ell(\widehat{C}^k_\ell \widehat{\eta}^k_{\mathrm{q},\ell} + \widehat{\eta}^k_{\mathrm{osc,q},\ell} + \widehat{\eta}^k_{\mathrm{iter},\ell}),
\end{aligned} \tag{10.6}$$

where we used the triangle inequality on $\ell_2(\mathbb{R}^{|\mathcal{V}_\ell|})$. Finally, we get $\widehat{C}^k_\ell = 1$ for the Zarantonello iteration since $A^{k-1}_{\mathrm{m},\ell} = A^{k-1}_{\mathrm{c},\ell} = \gamma$ in Ω in this case. □

A Equivalent assumptions on the nonlinear functions

In this section, we show some useful properties of the nonlinear functions a and ϕ. In particular, we show that inequalities (2.1) admit equivalent versions with the function ϕ defined in (2.4), preserving the same constants $a_{\rm c}$ and $a_{\rm m}$.

Proposition A.1 (Equivalent assumption on ϕ')**.** *Inequalities* (2.1) *are equivalent to the following ones: a.e. in* Ω*, for all* $r, s \in [0, \infty)$*,*

$$|\phi'(\cdot, r) - \phi'(\cdot, s)| \le a_{\rm c}|r - s|, \tag{A.1a}$$

$$(\phi'(\cdot, r) - \phi'(\cdot, s))(r - s) \ge a_{\rm m}(r - s)^2. \tag{A.1b}$$

Proof. Differentiating (2.4) gives, a.e. in Ω and for all $r \in [0, \infty)$,

$$\phi'(\cdot, r) = a(\cdot, r)r. \tag{A.2}$$

Thus, assuming and using (2.1) (with $\boldsymbol{x} = (r, 0, \ldots, 0)^{\rm t}$ and $\boldsymbol{y} = (s, 0, \ldots, 0)^{\rm t}$) together with (A.2) yields (A.1).

Reciprocally, assuming (A.1), we have in particular (with $s = 0$), using (A.2), a.e. in Ω and for all $r \in [0, \infty)$,

$$a_{\rm m} \le a(\cdot, r) \le a_{\rm c}. \tag{A.3}$$

We conclude by using the fact that for all $\boldsymbol{x}, \boldsymbol{y} \in \mathbb{R}^d$, and all $\alpha, \beta \in [0, \infty)$, we have

$$|\boldsymbol{x} - \boldsymbol{y}|^2 = (|\boldsymbol{x}| - |\boldsymbol{y}|)^2 + 2(|\boldsymbol{x}||\boldsymbol{y}| - \boldsymbol{x} \cdot \boldsymbol{y}), \tag{A.4a}$$

$$(\alpha\boldsymbol{x} - \beta\boldsymbol{y}) \cdot (\boldsymbol{x} - \boldsymbol{y}) = (\alpha|\boldsymbol{x}| - \beta|\boldsymbol{y}|)(|\boldsymbol{x}| - |\boldsymbol{y}|) + (\alpha + \beta)(|\boldsymbol{x}||\boldsymbol{y}| - \boldsymbol{x} \cdot \boldsymbol{y}), \tag{A.4b}$$

to obtain, a.e. in Ω and for all $\boldsymbol{x}, \boldsymbol{y} \in \mathbb{R}^d$,

$$\begin{aligned}
&|a(\cdot, |\boldsymbol{x}|)\boldsymbol{x} - a(\cdot, |\boldsymbol{y}|)\boldsymbol{y}|^2 \\
&\overset{\text{(A.4a)}}{=} (a(\cdot, |\boldsymbol{x}|)|\boldsymbol{x}| - a(\cdot, |\boldsymbol{y}|)|\boldsymbol{y}|)^2 + 2a(\cdot, |\boldsymbol{x}|)a(\cdot, |\boldsymbol{y}|)(|\boldsymbol{x}||\boldsymbol{y}| - \boldsymbol{x} \cdot \boldsymbol{y}) \\
&\overset{\text{(A.2)}}{=} (\phi'(\cdot, |\boldsymbol{x}|) - \phi'(\cdot, |\boldsymbol{y}|))^2 + 2a(\cdot, |\boldsymbol{x}|)a(\cdot, |\boldsymbol{y}|)(|\boldsymbol{x}||\boldsymbol{y}| - \boldsymbol{x} \cdot \boldsymbol{y}) \\
&\overset{\text{(A.1),(A.3)}}{\le} a_{\rm c}^2[(|\boldsymbol{x}| - |\boldsymbol{y}|)^2 + 2(|\boldsymbol{x}||\boldsymbol{y}| - \boldsymbol{x} \cdot \boldsymbol{y})] = a_{\rm c}^2|\boldsymbol{x} - \boldsymbol{y}|^2
\end{aligned}$$

and

$$\begin{aligned}
&(a(\cdot,|\boldsymbol{x}|)\boldsymbol{x} - a(\cdot, |\boldsymbol{y}|)\boldsymbol{y}) \cdot (\boldsymbol{x} - \boldsymbol{y}) \\
&\overset{\text{(A.4b)}}{=} (a(\cdot, |\boldsymbol{x}|)|\boldsymbol{x}| - a(\cdot, |\boldsymbol{y}|)|\boldsymbol{y}|)(|\boldsymbol{x}| - |\boldsymbol{y}|) + (a(\cdot, |\boldsymbol{x}|) + a(\cdot, |\boldsymbol{y}|))(|\boldsymbol{x}||\boldsymbol{y}| - \boldsymbol{x} \cdot \boldsymbol{y}) \\
&\overset{\text{(A.2)}}{=} (\phi'(\cdot, |\boldsymbol{x}|) - \phi'(\cdot, |\boldsymbol{y}|))(|\boldsymbol{x}| - |\boldsymbol{y}|) + (a(\cdot, |\boldsymbol{x}|) + a(\cdot, |\boldsymbol{y}|))(|\boldsymbol{x}||\boldsymbol{y}| - \boldsymbol{x} \cdot \boldsymbol{y}) \\
&\overset{\text{(A.1),(A.3)}}{\ge} a_{\rm m}[(|\boldsymbol{x}| - |\boldsymbol{y}|)^2 + 2(|\boldsymbol{x}||\boldsymbol{y}| - \boldsymbol{x} \cdot \boldsymbol{y})] = a_{\rm m}|\boldsymbol{x} - \boldsymbol{y}|^2,
\end{aligned}$$

hence (2.1). □

Proposition A.2 (Equivalent assumption on ϕ'')**.** *Inequalities* (A.1) *are equivalent to the facts that* ϕ' *is weakly differentiable and, a.e. in* Ω *and for a.e.* $r \in [0, \infty)$*,*

$$a_{\rm m} \le \phi''(\cdot, r) \le a_{\rm c}. \tag{A.5}$$

Proof. Assuming (A.1), since ϕ' is Lipschitz continuous thanks to (A.1a), ϕ' is weakly differentiable. Furthermore, defining the difference quotient, a.e. in Ω and for all $r, s \in [0, \infty)$, $r \neq s$, by

$$\tau(\cdot, r, s) := \frac{\phi'(\cdot, r) - \phi'(\cdot, s)}{r - s},$$

inequalities (A.1) are equivalent to the fact that, a.e. in Ω and for all $r, s \in [0, \infty)$, $r \neq s$,

$$a_{\rm m} \le \tau(\cdot, r, s) \le a_{\rm c}. \tag{A.6}$$

Hence, letting s tend to r in (A.6) gives (A.5).

On the other hand, assuming and integrating (A.5) gives, a.e. in Ω and for a.e. $r, s \in [0, \infty)$ with $r > s$,

$$a_{\rm m}(r - s) \le \phi'(\cdot, r) - \phi'(\cdot, s) \le a_{\rm c}(r - s), \tag{A.7}$$

and dividing (A.7) by $r - s$ gives (A.6), which becomes also true for $r < s$ by symmetry. □

Remark A.3 (Convexity)**.** *Under Assumption 2.1, inequality* (A.1b) *implies that* ϕ' *is nondecreasing, i.e.,* ϕ *is convex. Moreover, from* (A.2)*, we have, a.e. in* Ω *and for a.e.* $r \in [0, \infty)$*,*

$$\phi''(\cdot, r) = a(\cdot, r) + a'(\cdot, r)r. \tag{A.8}$$

B Spectral properties of the tensor product

Lemma B.1 (Spectral properties of the tensor product)**.** *The following holds:*

$$\mathrm{Spec}(\alpha \boldsymbol{I}_d + \beta \boldsymbol{A}) = \{\alpha\} + \beta\,\mathrm{Spec}(\boldsymbol{A}) \qquad \forall \alpha, \beta \in \mathbb{R},\ \forall \boldsymbol{A} \in \mathbb{R}^{d \times d}, \tag{B.1a}$$

$$\mathrm{Spec}(\boldsymbol{\xi} \otimes \boldsymbol{\xi}) = \{0, |\boldsymbol{\xi}|^2\} \qquad \forall \boldsymbol{\xi} \in \mathbb{R}^d,\ d > 1. \tag{B.1b}$$

Proof. We refer to [13] for details about the tools used in the following. Denoting $P_{\boldsymbol{A}}$ the characteristic polynomial of $\boldsymbol{A}$, we obtain (B.1a) by writing, for all $\lambda \in \mathbb{R}$,

$$P_{\alpha \boldsymbol{I}_d + \beta \boldsymbol{A}}(\alpha + \beta\lambda) = \det((\alpha + \beta\lambda)\boldsymbol{I}_d - (\alpha \boldsymbol{I}_d + \beta \boldsymbol{A})) = \beta^d \det(\lambda \boldsymbol{I}_d - \boldsymbol{A}) = \beta^d P_{\boldsymbol{A}}(\lambda).$$

Moving to (B.1b), since $(\boldsymbol{\xi} \otimes \boldsymbol{\xi})\boldsymbol{\tau} = (\boldsymbol{\xi} \cdot \boldsymbol{\tau})\boldsymbol{\xi}$ for all $\boldsymbol{\tau} \in \mathbb{R}^d$, $\dim(\mathrm{Ker}(\boldsymbol{\xi} \otimes \boldsymbol{\xi})) = \dim(\mathrm{Ker}(\langle \boldsymbol{\xi}, \cdot \rangle)) \geq d - 1$, i.e. $0 \in \mathrm{Spec}(\boldsymbol{\xi} \otimes \boldsymbol{\xi})$ with a multiplicity of at least $d - 1$. Thus, the sum of the eigenvalues of $\boldsymbol{\xi} \otimes \boldsymbol{\xi}$, being $\mathrm{tr}(\boldsymbol{\xi} \otimes \boldsymbol{\xi}) = |\boldsymbol{\xi}|^2$, is in $\mathrm{Spec}(\boldsymbol{\xi} \otimes \boldsymbol{\xi})$. Hence, 0 and $|\boldsymbol{\xi}|^2$ are the only elements of $\mathrm{Spec}(\boldsymbol{\xi} \otimes \boldsymbol{\xi})$, and we infer (B.1b). □

References

[1] S. Badia and F. Verdugo, *Gridap: an extensible finite element toolbox in Julia*, Journal of Open Source Software, 5 (2020), p. 2520, https://doi.org/10.21105/joss.02520.

[2] S. Bartels, *Numerical methods for nonlinear partial differential equations*, vol. 47 of Springer Series in Computational Mathematics, Springer, Cham, 2015, https://doi.org/10.1007/978-3-319-13797-1.

[3] S. Bartels and A. Kaltenbach, *Explicit and efficient error estimation for convex minimization problems*, 2022, https://doi.org/10.48550/ARXIV.2204.10745. ArXiv preprint 2204.10745.

[4] S. Bartels and M. Milicevic, *Primal-dual gap estimators for a posteriori error analysis of nonsmooth minimization problems*, ESAIM Math. Model. Numer. Anal., 54 (2020), pp. 1635–1660, https://doi.org/10.1051/m2an/2019074.

[5] L. Belenki, L. Diening, and C. Kreuzer, *Optimality of an adaptive finite element method for the p-Laplacian equation*, IMA J. Numer. Anal., 32 (2012), pp. 484–510, https://doi.org/10.1093/imanum/drr016.

[6] J. Blechta, J. Málek, and M. Vohralík, *Localization of the $W^{-1,q}$ norm for local a posteriori efficiency*, IMA J. Numer. Anal., 40 (2020), pp. 914–950, https://doi.org/10.1093/imanum/drz002.

[7] D. Boffi, F. Brezzi, and M. Fortin, *Mixed finite element methods and applications*, vol. 44 of Springer Series in Computational Mathematics, Springer, Heidelberg, 2013, https://doi.org/10.1007/978-3-642-36519-5.

[8] D. Braess and J. Schöberl, *Equilibrated residual error estimator for edge elements*, Math. Comp., 77 (2008), pp. 651–672, https://doi.org/10.1090/S0025-5718-07-02080-7.

[9] C. Carstensen, M. Feischl, M. Page, and D. Praetorius, *Axioms of adaptivity*, Comput. Math. Appl., 67 (2014), pp. 1195–1253, https://doi.org/10.1016/j.camwa.2013.12.003.

[10] A. L. Chaillou and M. Suri, *Computable error estimators for the approximation of nonlinear problems by linearized models*, Comput. Methods Appl. Mech. Engrg., 196 (2006), pp. 210–224, https://doi.org/10.1016/j.cma.2006.03.008.

[11] R. Cottereau, L. Chamoin, and P. Díez, *Strict error bounds for linear and nonlinear solid mechanics problems using a patch-based flux-free method*, Mechanics & Industry, 11 (2010), pp. 249–254, https://doi.org/10.1051/meca/2010049.

[12] R. Cottereau, P. Díez, and A. Huerta, *Strict error bounds for linear solid mechanics problems using a subdomain-based flux-free method*, Comput. Mech., 44 (2009), pp. 533–547, https://doi.org/10.1007/s00466-009-0388-1.

[13] C. W. Curtis, *Linear algebra*, Undergraduate Texts in Mathematics, Springer-Verlag, New York, fourth ed., 1993. An introductory approach.

[14] K. Deckelnick, G. Dziuk, and C. M. Elliott, *Computation of geometric partial differential equations and mean curvature flow*, Acta Numer., 14 (2005), pp. 139–232, https://doi.org/10.1017/S0962492904000224.

[15] P. Destuynder and B. Métivet, *Explicit error bounds in a conforming finite element method*, Math. Comp., 68 (1999), pp. 1379–1396, https://doi.org/10.1090/S0025-5718-99-01093-5.

[16] P. Deuflhard, *Newton methods for nonlinear problems*, vol. 35 of Springer Series in Computational Mathematics, Springer, Heidelberg, 2011, https://doi.org/10.1007/978-3-642-23899-4. Affine invariance and adaptive algorithms, First softcover printing of the 2006 corrected printing.

[17] L. El Alaoui, A. Ern, and M. Vohralík, *Guaranteed and robust a posteriori error estimates and balancing discretization and linearization errors for monotone nonlinear problems*, Comput. Methods Appl. Mech. Engrg., 200 (2011), pp. 2782–2795, https://doi.org/10.1016/j.cma.2010.03.024.

[18] A. Ern and J.-L. Guermond, *Theory and practice of finite elements*, vol. 159 of Applied Mathematical Sciences, Springer-Verlag, New York, 2004, https://doi.org/10.1007/978-1-4757-4355-5.

[19] A. Ern, I. Smears, and M. Vohralík, *Discrete p-robust* $\boldsymbol{H}(\mathrm{div})$*-liftings and a posteriori estimates for elliptic problems with* H^{-1} *source terms*, Calcolo, 54 (2017), pp. 1009–1025, https://doi.org/10.1007/s10092-017-0217-4.

[20] A. Ern and M. Vohralík, *Adaptive inexact Newton methods with a posteriori stopping criteria for nonlinear diffusion PDEs*, SIAM J. Sci. Comput., 35 (2013), pp. A1761–A1791, https://doi.org/10.1137/120896918.

[21] A. Ern and M. Vohralík, *Stable broken* H^1 *and* $H(\mathrm{div})$ *polynomial extensions for polynomial-degree-robust potential and flux reconstruction in three space dimensions*, Math. Comp., 89 (2020), pp. 551–594, https://doi.org/10.1090/mcom/3482.

[22] R. E. Ewing, *Finite element methods for nonlinear flows in porous media*, vol. 51, 1985, pp. 421–439, https://doi.org/10.1016/0045-7825(85)90041-6. FENOMECH ’84, Part I, II (Stuttgart, 1984).

[23] F. Févotte, A. Rappaport, and M. Vohralík, *Adaptive regularization, discretization, and linearization for nonsmooth problems based on primal-dual gap estimators*, Comput. Methods Appl. Mech. Engrg., 418 (2024), p. 116558, https://doi.org/10.1016/j.cma.2023.116558.

[24] G. Gantner, A. Haberl, D. Praetorius, and B. Stiftner, *Rate optimal adaptive FEM with inexact solver for nonlinear operators*, IMA J. Numer. Anal., 38 (2018), pp. 1797–1831, https://doi.org/10.1093/imanum/drx050.

[25] E. M. Garau, P. Morin, and C. Zuppa, *Convergence of an adaptive Kačanov FEM for quasi-linear problems*, Appl. Numer. Math., 61 (2011), pp. 512–529, https://doi.org/10.1016/j.apnum.2010.12.001.

[26] M. Guo, W. Han, and H. Zhong, *Legendre-Fenchel duality and a generalized constitutive relation error*. ArXiv preprint 1611.05589, 2016, https://arxiv.org/abs/1611.05589.

[27] A. Haberl, D. Praetorius, S. Schimanko, and M. Vohralík, *Convergence and quasi-optimal cost of adaptive algorithms for nonlinear operators including iterative linearization and algebraic solver*, Numer. Math., 147 (2021), pp. 679–725, https://doi.org/10.1007/s00211-021-01176-w.

[28] W. Han, *A posteriori error analysis for linearization of nonlinear elliptic problems and their discretizations*, Math. Methods Appl. Sci., 17 (1994), pp. 487–508, https://doi.org/10.1002/mma.1670170702.

[29] W. Han, *A posteriori error analysis via duality theory*, vol. 8 of Advances in Mechanics and Mathematics, Springer-Verlag, New York, 2005. With applications in modeling and numerical approximations.

[30] P. Heid, D. Praetorius, and T. P. Wihler, *Energy contraction and optimal convergence of adaptive iterative linearized finite element methods*, Comput. Methods Appl. Math., 21 (2021), pp. 407–422, https://doi.org/10.1515/cmam-2021-0025.

[31] P. Heid and T. P. Wihler, *On the convergence of adaptive iterative linearized Galerkin methods*, Calcolo, 57 (2020), pp. Paper No. 24, 23, https://doi.org/10.1007/s10092-020-00368-4.

[32] J. Hiriart-Urruty and C. Lemarechal, *Convex Analysis and Minimization Algorithms I: Fundamentals*, Grundlehren der mathematischen Wissenschaften, Springer Berlin Heidelberg, 1996.

[33] P. Houston, E. Süli, and T. P. Wihler, *A posteriori error analysis of hp-version discontinuous Galerkin finite-element methods for second-order quasi-linear elliptic PDEs*, IMA J. Numer. Anal., 28 (2008), pp. 245–273.

[34] C. T. Kelley, *Iterative methods for linear and nonlinear equations*, vol. 16 of Frontiers in Applied Mathematics, Society for Industrial and Applied Mathematics (SIAM), Philadelphia, PA, 1995, https://doi.org/10.1137/1.9781611970944. With separately available software.

[35] K.-Y. Kim, *A posteriori error estimators for locally conservative methods of nonlinear elliptic problems*, Appl. Numer. Math., 57 (2007), pp. 1065–1080, https://doi.org/10.1016/j.apnum.2006.09.010.

[36] P. Ladevèze and D. Leguillon, *Error estimate procedure in the finite element method and applications*, SIAM J. Numer. Anal., 20 (1983), pp. 485–509.

[37] P. Ladevèze and N. Moës, *A posteriori constitutive relation error estimators for nonlinear finite element analysis and adaptive control*, in Advances in adaptive computational methods in mechanics (Cachan, 1997), vol. 47 of Stud. Appl. Mech., Elsevier Sci. B. V., Amsterdam, 1998, pp. 231–256, https://doi.org/10.1016/S0922-5382(98)80013-5.

[38] M. G. Larson and A. J. Niklasson, *A conservative flux for the continuous Galerkin method based on discontinuous enrichment*, Calcolo, 41 (2004), pp. 65–76, https://doi.org/10.1007/s10092-004-0084-7.

[39] K. Mitra and M. Vohralík, *Guaranteed, locally efficient, and robust a posteriori estimates for nonlinear elliptic problems in iteration-dependent norms. An orthogonal decomposition result based on iterative linearization.* HAL Preprint 04156711, submitted for publication, 2023, https://hal.inria.fr/hal-04156711.

[40] P. Neittaanmaki and S. Repin, *A posteriori error identities for nonlinear variational problems*, Ann. Acad. Rom. Sci. Ser. Math. Appl., 7 (2015), pp. 157–172.

[41] S. Repin, *A posteriori estimates for partial differential equations*, vol. 4 of Radon Series on Computational and Applied Mathematics, Walter de Gruyter GmbH & Co. KG, Berlin, 2008, https://doi.org/10.1515/9783110203042.

[42] J. L. Vázquez, *An introduction to the mathematical theory of the porous medium equation*, in Shape optimization and free boundaries (Montreal, PQ, 1990), vol. 380 of NATO Adv. Sci. Inst. Ser. C: Math. Phys. Sci., Kluwer Acad. Publ., Dordrecht, 1992, pp. 347–389.

[43] F. Verdugo and S. Badia, *The software design of Gridap: a finite element package based on the Julia JIT compiler*, Computer Physics Communications, 276 (2022), p. 108341, https://doi.org/10.1016/j.cpc.2022.108341.

[44] E. H. Zarantonello, *Solving Functional Equations by Contractive Averaging*, Tech. Report 160, Mathematics Research Center, United States Army, University of Wisconsin, 1960.

[45] E. Zeidler, *Nonlinear Functional Analysis and Its Applications. II/B: Nonlinear Monotone Operators*, no. XV, 1992, https://doi.org/10.1007/978-1-4612-0981-2.